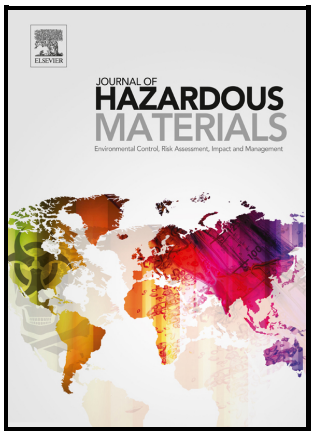

Plastisphere on microplastics: *In situ* assays in an estuarine environment

A.D. Forero López, L.I. Brugnoni, B. Abasto, G.N. Rimondino, V.L. Lassalle, M.G. Ardusso, M.S. Nazzarro, A.M. Martinez, C.V. Spetter, F. Biancalana, Fernández Severini

PII: S0304-3894(22)01530-8

DOI: https://doi.org/10.1016/j.jhazmat.2022.129737

Reference: HAZMAT129737

To appear in: *Journal of Hazardous Materials*

Received date: 28 April 2022
Revised date: 27 July 2022
Accepted date: 7 August 2022

Please cite this article as: A.D. Forero López, L.I. Brugnoni, B. Abasto, G.N. Rimondino, V.L. Lassalle, M.G. Ardusso, M.S. Nazzarro, A.M. Martinez, C.V. Spetter, F. Biancalana and Fernández Severini, Plastisphere on microplastics: *In situ* assays in an estuarine environment, *Journal of Hazardous Materials,* (2022) doi:https://doi.org/10.1016/j.jhazmat.2022.129737

Plastisphere on microplastics: *In situ* assays in an estuarine environment.

A.D. Forero López[1*], L.I. Brugnoni[2], B. Abasto[1,3], G.N. Rimondino[4], V.L. Lassalle[3,5], M.G. Ardusso[1], M.S. Nazzarro[6], A.M. Martinez[3], C.V. Spetter[1,3], F. Biancalana[1] and M.D. Fernández Severini[1*]

[1]*Instituto Argentino de Oceanografía (IADO), CONICET/UNS, CCT-Bahía Blanca, Camino La Carrindanga, km 7.5, Edificio E1, B8000FWB, Bahía Blanca, Buenos Aires, Argentina.*

[2]*Instituto de Ciencias Biológicas y Biomédicas del Sur, INBIOSUR (UNS-CONICET), San Juan 670, 8000 Bahía Blanca, Argentina.*

[3]*Departamento de Química, Universidad Nacional del Sur (UNS), Avenida Alem 1253, B8000CPB, Bahía Blanca, Buenos Aires, Argentina.*

[4]*Instituto de Investigaciones en Fisicoquímica de Córdoba (INFIQC), Departamento de Fisicoquímica, Facultad de Ciencias Químicas, Universidad Nacional de Córdoba, Ciudad Universitaria X5000HUA, Córdoba, Argentina.*

[5]*Instituto Nacional de Química del Sur (INQUISUR), CONICET/UNS, CCT-Bahía Blanca, Avenida Alem 1253, B8000CPB, Bahía Blanca, Buenos Aires, Argentina.*

[6]*Instituto de Física Aplicada "Dr. Jorge Andres Zgrablich" (INFAP),CCT-CONICET- San Luis, Almte. Brown 869, D5700ANU, San Luis, Argentina.*

* Corresponding author at: Instituto Argentino de Oceanografía (IADO), CONICET/UNS, CCT-BB Camino La Carrindanga, km 7.5, Edificio E1, B8000FWB, Bahía Blanca, Pcia. de Bs. As., Argentina. E- mail address: aforero@iado-conicet.gob.ar; (A.D. Forero López) and melisafs@criba.edu.ar (M.D. Fernández Severini).

Highlights

- **Pathogenic bacteria were identified on the Ny and PS-microplastic surfaces.**
- **Superficial weathering and leaching of TiO_2 from Ny Microplastics were evidenced.**
- **The crystallinity of Ny-microplastics decreased during the assay.**
- **High Cr, Mn, and Zn levels were detected on the microplastic surface biofilms.**

Abstract

In this study, the influence of the plastisphere on metals accumulation and weathering processes of polystyrene (PSMPs) and nylon microplastics (NyMPs) in polluted waters during a 129 day-assay were studied. MPs were characterized through scanning electron microscopy (SEM) with Energy dispersive X-ray (EDX), X-ray diffraction (XRD), attenuated total reflectance Fourier transformed infrared (ATR-FTIR) spectroscopy, contact angle, and thermogravimetric analysis (TGA). Also Cr, Mn, Zn, Cd, Pb, and Cu in the plastisphere on MPs were analyzed during the assay. Potentially pathogenic *Vibrio*, *Escherichia coli*, and *Pseudomonas* spp. were abundant in both MPs. Ascomycota fungi (*Phona* s.l., *Alternaria* sp., *Penicillium* sp., and *Cladosporium* sp.), and yeast, were also identified. NyMPs and PSMPs exhibited a decrease in the contact angle and increased their weights. SEM/EDX showed weathering signs, like surface cracks and pits, and leaching TiO_2 pigments from NyMPs after 42 days. XRD displayed a notorious decrease in NyMPs crystallinity, which could alter its interaction with external contaminants. Heavy metal accumulation on the plastisphere formed on each type of MPs increased over the exposure time. After 129 days of immersion, metals concentrations in the plastisphere on MPs were in

the following order Cr > Mn > Zn > Cu > Pb > Cd, demonstrating how the biofilm facilitates metal mobilization. The results of this study lead to a better understanding of the impact of marine plastic debris as vectors of pathogens and heavy metals in coastal environments.

Graphical abstract

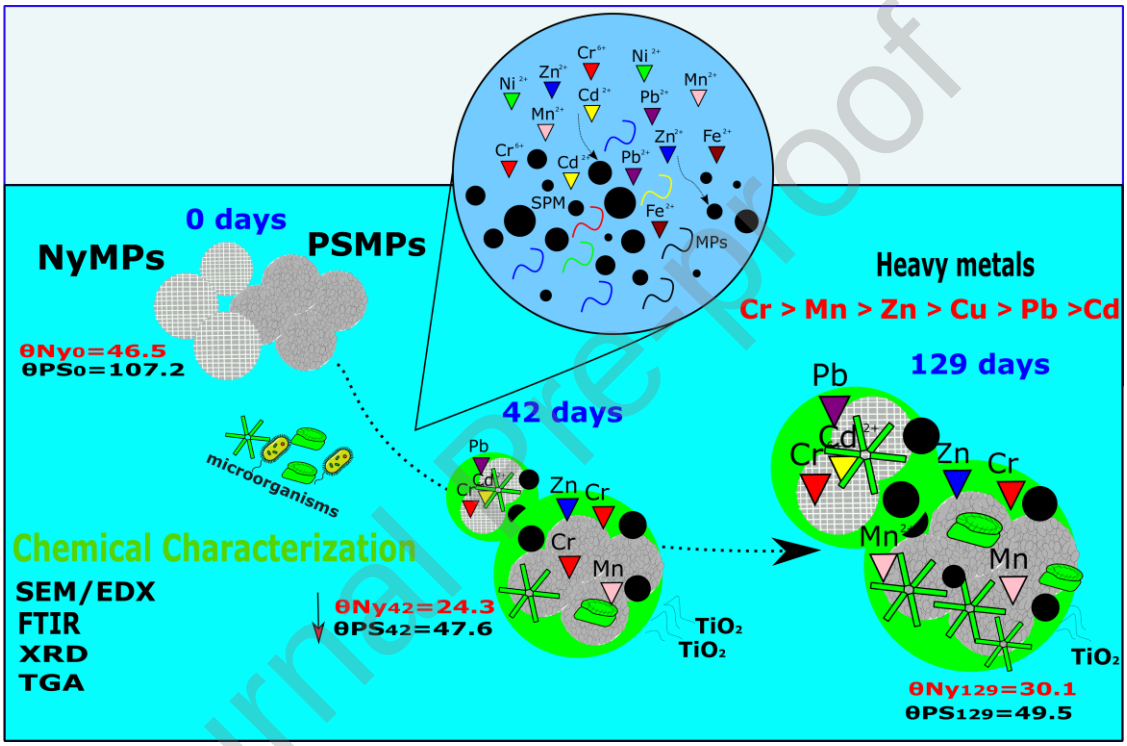

Keywords:

Surface degradation; Heavy metals; Biofilms; Pathogens; Pollution

"Environmental Implication"

The manuscript is of environmental relevance because it studies the presence of hazardous materials like microplastics and heavy metals in a marine ecosystem and their interactions with microorganisms of human health implications. Microplastics produce several impacts

on the environment and one of them is the formation of the plastisphere: microorganisms that colonize plastics. This study showed that MPs surfaces acted as new niches for heterotrophic microorganisms like pathogenic bacteria and favored the adsorption of heavy metals, with potential migration through the water to other marine ecosystems. Thus, the plastisphere plays as a metal vector with impacts on both aquatic biota and humans, through the food webs.

1. Introduction

Plastics are used for several purposes, making our life easier; however, the excessive use of these materials has generated large volumes of waste in the environment. Plastic waste after long-term exposure to environmental conditions such as mechanical abrasion, wind effects, ultraviolet radiation, chemical actions, and biodegradation (Wang et al. 2017; Paul-Pont et al. 2018; Kumar et al. 2021) breaks down into small pieces (micro/nanoplastics). The presence of microplastics (MPs, plastic pieces smaller than 5 mm) and nanoplastics (PNPs, particles smaller than 1 μm), around the world is a critical issue of great concern because they are degradation-resistant and have the ability to absorb, accumulate, and transport other contaminants and pathogenic organisms present in the environment (Thompson, 2015; Pizarro-Ortega et al. 2022; Forero-López et al. 2022). Furthermore, the presence of MPs/PNPs has been reported in aquatic, terrestrial, and air environments and in the organisms that inhabit them (Horton et al. 2017; Gasperi et al. 2018; Guo et al. 2020; Ocean, 2020). These plastic particles pose an ecological and toxicological threat (Sussarellu et al. 2016; Bhagat et al. 2020; Payton et al. 2020) because they can release additives (Deng et al. 2018; Luo et al. 2020) therefore, impacting on organisms causing cellular damage through oxidative stress, reduced fertility and alteration of their metabolism, among others (Cole et

al. 2015; Sussarellu et al. 2016; Payton et al. 2020). Moreover, within the ecological ones, MPs as a substrate, may favor the growth of some microbiological species, generating critical changes in the food chains as well as in the phenology and survival of some species (Nava and Leoni, 2021; Learn et al. 2021; Li et al. 2021).

Like any material that enters aquatic environments, MPs rapidly become biofouled, i.e., colonized by living organisms that accumulate over time. These organisms are microbial communities (biofilms) composed of diverse bacteria, single-celled algae, diatoms, fungi, and protozoa (Rummel et al. 2017; Miao et al. 2021; Kalčíková and Bundschuh, 2021). The plastisphere is the term used to mention the microbial biofilms associated with plastics or MPs (Zettler et al. 2013). These microorganisms that form the plastisphere, develop on the surface and sometimes even inside plastics depending on the structure of the polymer (Kettner et al. 2017; Amaral-Zettler et al. 2020). The prokaryotic and eukaryotic groups that live in plastic biofilms can also include pathogenic (Kirstein et al. 2016; Amaral-Zettler et al. 2020) or hydrocarbon-degrading organisms (Delacuvellerie et al. 2019; Oberbeckmann & Labrenz, 2020; Zhang et al. 2021). In recent years, the potential hazards of microbial communities from biofilms on MPs surface have received increasing attention. Some studies have shown that MPs surfaces are enriched with certain pathogenic bacteria (Kirstein et al. 2016; Wu et al. 2019), such as *Vibrio* and *Pseudomonas*, and could also be a reservoir for faecal indicator organisms, such as *E. coli*.

As previously mentioned, MPs/PNPs can absorb, accumulate, and transport other pollutants present in the aquatic environment (Wang et al. 2017; Tang et al. 2020 and 2021; Gao et al. 2021; Liu et al. 2022; Xie et al. 2022). Moreover, it has also been evidenced that the plastisphere formed on the plastic surface and the weathering degree plays an important

role in the sorption processes between plastic particles and pollutants such as heavy metals (Richard et al. 2019; Gao et al. 2021; Liu et al. 2022; Wu et al. 2022). Likewise, laboratory studies have also demonstrated that the physicochemical variables (e.g., salinity, organic matter dissolved, pH), chemical speciation of metal ions, type of polymer and its physicochemical properties (e.g., polarity, functional groups, specific surface area, and crystallinity), affect MPs sorption behavior (Tang et al. 2020 and 2021; Li et al. 2022). However, the nature of the multiple sorption mechanisms that occur on MPs surface and in the microparticle body is still unclear (Binda et al. 2021).

Furthermore, most publications have studied the growth of biofilm and the influence of the plastisphere on the accumulation of heavy metals as well as the weathering process of MPs under laboratory conditions (e.g., Gao et al., 2021; Li et al. 2022; Wu et al. 2022). However, few studies have been performed *in situ*. This is mainly due to the multiple factors that may affect the results and can't be controlled. For example, weather and the physico-chemical variables constantly change, making natural environments dynamic and complex. Anyway, in situ experiments help better understand the magnitude of microplastic pollution on the environment. They provide a more accurate and complete overview of the influence of all-environmental variables on the sorption behavior and aging of MPs in the presence of other pollutants. Among the few publications with *in situ* experiments ,researchers have studied the growth of biofilm and the composition of the microbial community on the surface of MPs. It is also of great interest its possible impact on the biogeochemical cycles (e.g., phosphorus, nitrogen and carbon) (Arias-Andrés et al. 2018; Chen et al. 2020; Deng et al. 2021), and accumulation and speciation distribution of heavy metals on polystyrene (Richards et al. 2019; Xie et al. 2022). However, the influence of biofilm growth on the

heavy metal accumulation in MPs and how the presence of biofilm affects their aging in estuarine environments has not been studied yet. Under this context, the goals of the present study are: 1) to conduct *in situ* assays to analyze changes in the formation of the plastisphere as well as the structural and chemical changes in MPs (polystyrene and nylon) submerged in marine waters from the Bahía Blanca Estuary for 129 days, 2) analyze metals adsorbed on MPs and 3) analyze the surrounding water through their physicochemical characteristics.

2. Material and methods

2.1 Study Area

The *in situ* assays were conducted during Summer-Autumn (129 days, January-June 2021) in The Bahía Blanca Estuary (BBE) (38°55.5′10.52″ S; 62°03′20.75″ W) situated in the Southwestern Atlantic Ocean, Buenos Aires province (Argentina) (**Figure S1.**). It is a highly polluted estuary with several chemical and petrochemical industries, sewage discharges, and intense marine traffic (Fernandez-Severini et al. 2018). However, it is also a Natural Reserve with emblematic species of ecological importance as the intertidal crab (*Neohelice granulata*), the Olrog's Gull *(Larus atlanticus)*, and del Plata dolphin (*Pontoporia blainviellei*) (Petracci and Sotelo, 2013; Speake et al. 2018). Some studies in this estuary have reported relatively high concentrations of MPs in surface waters (Fernandez-Severini et al. 2019; Forero-López et al. 2021a and c), in sediments (Diaz Jaramillo et al. 2021) as well as in aquatic organisms such as crabs (Villagran et al. 2020; Truchet et al. 2022b), oysters (Fernandez-Severini et al. 2019), and shrimps (Fernandez-Severini et al. 2020). High levels of Cd, Pb, Ni, and Cr have also been noted in Suspended Particulate Matter (SPM) (Fernandez et al. 2017 and 2018; Forero López et al. 2021b), and mesozooplankton (Fernandez-Severini et al. 2011; Villagran et al. 2019) of the BBE. The *in situ* assays were

carried out at Cuatrero Port (CP), which is located in the innermost part of the BBE. CP is an artisanal and recreational fishery port with an average depth of 7 m and vertically homogeneous physicochemical variables in the water column (Freije et al. 2008; Forero Lopez et al. 2021a) with the highest primary production of the system (Carbone et al. 2016; Guinder et al. 2013 and 2015).

2.2 *In situ* assays

Virgin nylon (Ny) disks and polystyrene (PS) spheres (4.70 ± 0.15 and 2.43 ± 0.43 mm diameter, respectively) were used as MPs models for the experiments. Ny is one the most common types of MPs found in the surface waters of the BBE (Forero Lopez et al. 2021a and c) and near this estuary (Truchet et al. 2021b), while PS is widely employed in contaminant absorption studies under laboratory conditions (Lu et al. 2018; Liu et al. 2019; Guan et al. 2020; Gao et al. 2021). In addition, MPs tend to be hydrophobic materials and their contact angle depends on the nature of the material surface (e.g. rugosity) and the interaction between interphases (solid/liquid/gas) (Mahltig, 2016). Three hundred PS microspheres and 100 disks of Ny were placed into each yellow nylon bag (mesh size of 30 μm) and inside stainless steel tea balls (4.5 cm diameter with size, porous mesh 1.25 mm) to exclude benthic and macroplankton organisms. A total of 28 balls were attached to a stainless steel chain with 400 MPs each. This chain was always under water (2 meters deep) in a dock at the BBE (**Figure 1a-c).** Every 14 days, two or three tea balls were collected from the water with the nylon bags containing MPs. They were placed in a sterile polypropylene container of 125 mL, immediately refrigerated in a cool box (at approx. 5ºC) and transported to the laboratory for microbiologic (plastisphere) analysis, chemistry characterization, and heavy metal analysis in the plastisphere. Finally, surface water samples

were collected manually for the analysis of metals in the dissolved fraction, using 1.5 L polyethylene-terephthalate (PET) bottles previously conditioned HNO_3 following the methodology described by Villagran et al. (2019).

Figure 1. (a) Satelital photograph of the assay area at Cuatreros Port (CP). (b) Schematic drawing of the assay in surface waters of Cuatreros Port (CP), at the Bahía Blanca Estuary (BBE) and (c) photograph of stainless steel tea balls with MPs inside a Nylon bag (small insert).

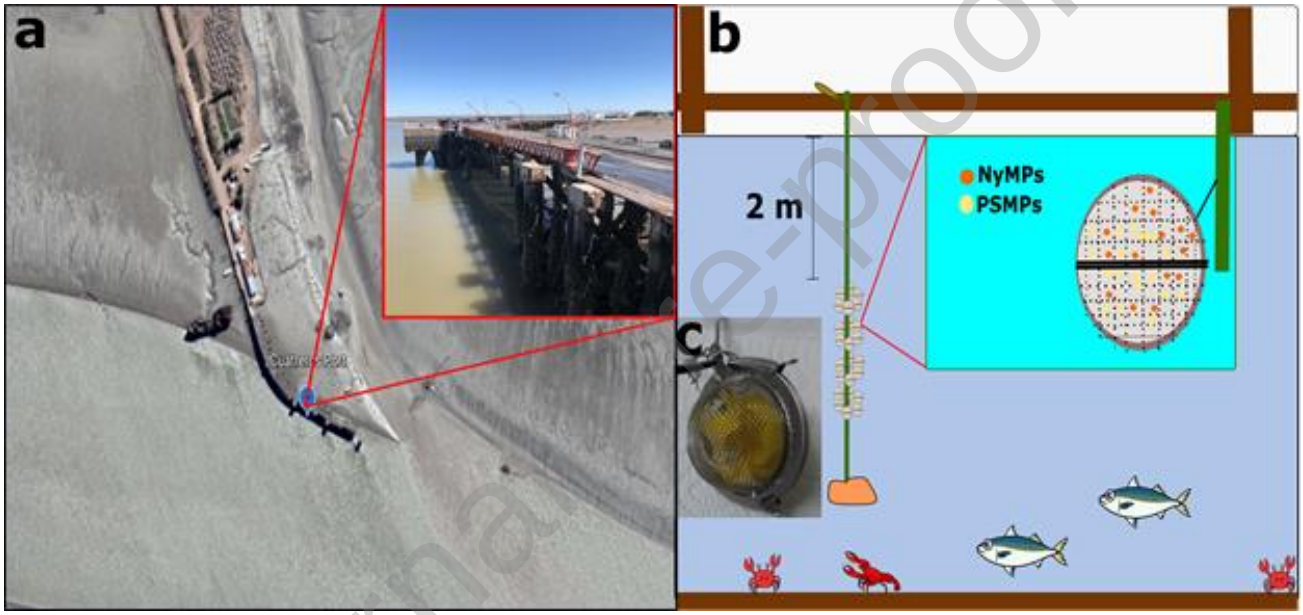

2.3 Chemical characterization of MPs

During the cleaning and preparation of the samples for the respective instrumental chemical characterization, cotton lab coats, clothing, and nitrile gloves were used. MPs (Ny and PS) were characterized at different assay times: 0, 42, and 129 days (final time) by ATR-FTIR spectroscopy, X-ray diffraction analysis (XRD), Scanning Electron Microscope (SEM) coupled with an Energy Dispersive X-ray analyzer (EDX), Thermal Gravimetric Analysis (TGA), and contact angle (θ) measurements.

2.3.1 ATR-FTIR analyses

Each type of MPs was cleaned with abundant distilled water for the removal of biomass and sonicated for 20 min (repeating 3 times) and dried to constant weight (50 °C). The biofilm removal and MPs clean up are performed to avoid the confusion of the spectral signatures of contamination with the plastic oxidation (Sandt et al. 2021). MPs were dried to constant weight and then weighed on an analytical balance (OHAUS, Adventurer™) to calculate their weight gain percentage. MPs (Ny and PS) were characterized by ATR-FTIR spectroscopy using a Nicolet iS5 spectrometer (Thermo Fisher) equipped with an iD7 ATR module. Spectra were recorded between 500 cm^{-1} to 4000 cm^{-1} with 4 cm^{-1} resolution. The equipment was employed to ascertain the functional groups present in MPs.

2.3.2 XRD analyses

Once that MPs were cleaned according to the methodology mentioned above in section 2.3.1. The change of crystalline structure of each type of MPs was identified with a PANalytical Empyrean 3 diffractometer with an Ni-filtered CuKα radiation and a PIXcel^{3D} detector. The equipment was operated at a voltage of 45 kV and a current of 40 mA following the methodology described by De la Torre et al. (2022). The data were collected using a continuous scan mode with a divergence slit of 1/2 ° and a scan angular speed of 0.042 °/s for the 2Θ range 10 °≤ 2Θ ≤ 80 °.

2.3.3 SEM/EDX analyses of the plastisphere on MPs

2.3.3.1 Morphological change of MPs

The change in the morphological and elemental composition of MPs was performed by SEM (Zeiss Evo Ma10) coupled with EDX (EDAX 9600). MPs were placed over the aluminum tape on an SEM holder and gold-coated. Then, the samples were analyzed by the electronic microscope, using an accelerating voltage of 20 kV with a working distance of 8–9 mm following the methodology described by Forero-Lopez et al. (2020).

2.3.3.2 Biofilm formed on the surface of MPs

The biofilms formed on the surface of MPs were characterized by SEM/EDX. The samples were placed in 2.5% glutaraldehyde for 24 h at 4 °C and then they were washed three times with a phosphate buffer (0.1 M, pH 7.2) and dehydrated by critical point drying (E3000, Polaron Instruments, Hatfield, PA) according to the methodology detailed in Agustin et al. (2018). Then, MPs were coated with a thin Au layer before analysis, following the conditions described in Forero López et al. (2021a).

2.3.4 TGA analyses

The weight loss and thermal stability measurements of each type of MPs at o and 129 days of immersion were performed utilizing Thermal Gravimetric Analysis (TGA) was used (SDT-Q600 Instrument Simultaneous). Between 3 and 5 mg of each MPs previously cleaned were scanned at temperatures between 30 and 800 °C with a heating rate of 10 °C min^{-1} in a nitrogen atmosphere.

2.3.5 Contact angle (θ) measurements

Finally, the contact angle **(θ)** measurements of MPs samples were performed in order to characterize the change of the hydrophobicity in their surfaces, before and after the experiment, using a Krüss DSA25 Expert analyzer. The measurements were performed at 23 °C using a 5 μL droplet of triply distilled water. Each measurement for each type of MPs was done in triplicate with variability within ± 5%.

2.4 Environmental variables

Environmental parameters such as pH, temperature, salinity, turbidity, and dissolved oxygen (DO) of surface water were measured *in situ* with a PCE-PHD1 multi-sensor every 14 days during the development of the experiment. The water samples for the analysis of soluble reactive phosphorus (SRP), total particulate nitrogen (TPN), chlorophyll-a (Chl-*a*) and phaeopigments (*phae)*, suspended particulate matter (SPM), total particulate carbon (TPC), and dissolved organic matter (DOM) were collected in previously conditioned PET bottles, following the methodology in Holm-Hansen et al. (1965), Spetter et al. (2015), and Garzón-Cardona et al. (2021), respectively.

Water samples for determination of SRP (as PO_4^{3-}, μM), TPN, TPC, and DOM, were immediately filtered through Sartorius glass fiber grade F (MGF, with a diameter 47 mm and pore size of 0.7 μm) membranes previously muffled (450 ± 50 °C, 1h). Water samples for SRP analyses were stored in plastic bottles and for DOM in glass tubes muffled (450 ± 50 °C, 1h), and frozen (-20 °C) until further analysis in the laboratory. Particulate material (volume > 250 mL) was preserved in foil envelopes and kept in the freezer (- 20 °C), then freeze-dried and dry preserved until analysis. SRP concentration was determined following the method of Murphy and Riley (1962) modified by Eberlein and Kattner (1987) using a UV-Vis spectrophotometer (Jenway 6715) with a detection limit of 0.10 μM. TPN

($mg.L^{-1}$) and TPC ($mg.L^{-1}$) levels were determined using an Elemental Analyzer Exeter (Analytical CE-440) with a detection limit of 1 µg N and 1 µg.C. Water samples for Chl-*a* concentration and phaeopigment contents ($\mu g.L^{-1}$) were also filtered through Sartorius glass fiber grade F (with a diameter 47 mm and pore size of 0.7 µm) membranes, kept away from light in the freezer (-20 °C). In order to spectrophotometrically determine Chl-*a* and *phae* APHA (1998) methodology was used. On the other hand, to determine SPM concentrations ($mg.L^{-1}$) in water samples, 750 mL of water were vacuum filtered through nitrocellulose filters (0.45 µm pore size, Millipore). Then, the filters with SPM were dried at 50 ± 5 °C to constant weight on an analytical balance and stored in a desiccator until further analysis. Finally, for characterizing DOM, a Shimadzu RF6000 spectrofluorometer was employed with a 150W xenon lamp and a quartz cell (1 cm). The intensity of the Raman peak was regularly tested, and Milli-Q water was used as a reference for this analysis. The estimation of dissolved humic-like fluorophores ($FDOM_M$ and $FDOM_C$) and protein-like fluorophores ($FDOM_T$ and $FDOM_B$) were determined using the wavelength at $Ex/Em_{(FDOMM)}$:310/380 nm, $Ex/Em_{(FDOMc)}$:350/440 nm; $Ex/Em_{(FDOMT)}$:270/330 nm, and $Ex/Em_{(FDOMB)}$: 260/300 nm, respectively, which were proposed by Coble (1996). Finally, three fluorescence indices (fluorescence index = FIX, humification index = HIX, and biological index = BIX) were used to assess possible sources and the diagenetic state of DOM substances and were calculated following the methodology used by Huguet et al. (2009) and Garzón-Cardona et al. (2021).

2.5. Quality assurance (QA) and quality control (QC)

All the materials for metal analysis in the plastisphere on MPs and dissolved fractions in the water column were soaked in ultrapure acid (5% HNO_3, 48 h) and rinsed several times with ultrapure water before use, following the methodology described by Villagrán et al. (2019). The metal concentrations in the plastisphere of MPs and dissolved fraction in water column were analyzed by duplicate with an ICP-OES Optima 2100 DV Perkin Elmer. The detection limit of the method (MDL) for Cr, Mn, Cu, Zn, Cd, and Pb were 0.06, 0.23, 0.09, 0.11, 0.03, and 0.04 $\mu g.g^{-1}$, respectively. For details of MDL calculation formula, see Federal Register (1984). For analytical quality control, reagent blanks, certified reference materials (CRMs [plankton, Certified Reference Material BCR No414, IRMM, Geel, Belgium]), and analytical grade reagents were used. The blanks, reference material, and solutions were also prepared with ultrapure water (Villagrán et al. 2019). The recovery percentages for all heavy metals in CRM were higher than 90% (**Table S1 Supl. Material**).

2.6 Heavy metal analyses in the environment and the plastisphere on MPs

For metal analysis in PS and NyMPs samples, MPs were rinsed with filtered (0.45 μm, nitrocellulose filter 47 mm diameter) distilled water and dried for 56 h in previously conditioned Petri dishes (APHA, 1998). 0.03 g of NyMPs (50 microdisks) and 0.06 g PSMPs (145 microspheres) with their respective duplicate (PS spheres and Ny disks) were acid-digested (70% HNO_3 ultrapure and 70% $HClO_4$ ultrapure, 5:1, 110 ± 10 °C) in a glycerine bath for 56 h to obtain an extract of about 1 mL. Each of these extracts was diluted with 0.7% HNO_3 to final volume (10.00 mL) according to the description of Villagrán et al. (2019). The same procedure was performed for the blank reagents used for digestion and virgin MPs blanks.

2.7 Microbiological analyses

Attached biofilm was dislodged by placing 1 g of plastic pieces into test tubes with 9 mL sterile water and 5 glass beads (5 mm diameter). Then, the test tubes with the samples were sonicated for 2 min at 20 ºC (Digital Ultrasonic Cleaner, PS-10A) and vortexed at full speed for another 2 min before serial dilutions were prepared. 100 µL from each dilution were plated on PCA (Plate Count Agar, Merck), YGC agar (Biokar) and King's B agar (*Pseudomonas* agar F, Difco) previously prepared with sterile natural seawater collected from CP, to investigate the number of culturable heterotrophic bacteria, molds and yeast, and fluorescent P*seudomonas*, respectively. The plates were incubated at 25 °C for 1 week. For *Vibrio* spp. investigation, 1 g of samples were incubated in alkaline peptone water (APW) (1% NaCl, pH 8.6) for 6-8 h at 35 °C. The enrichments were then streaked onto thiosulphate-citrate-bile-salt-agar (TCBS) plus 2% NaCl and incubated for 24–48 h at 35 °C. The suspected colony types (yellow and green) were picked out, streaked onto nutrient agar plus 2% NaCl to obtain pure cultures, and screened for cytochrome oxidase.

Total coliforms and *E. coli* were enumerated by the most probable number method (MPN) using the standard three-tube method of ten-fold dilution incubated for 24-48 h at 35 °C and 44.5 °C, respectively. Tubes displaying gas in the Durham tube accompanied by a yellow color of the medium represent a positive test for total coliforms (positive tubes). The results were reported as $MPN.g^{-1}$. A portion of positive cultures at 35 °C was transferred and incubated at 44.5 °C to further investigate *E. coli.* McConkey Broth (Oxoid) was used as cultural media. A loop of positive cultures at 44.5 °C were streaked onto PCA to obtain pure cultures, and identified by biochemical tests.

For the qualitatively analyzed biota, associated with both types of MPs, samples were fixed in buffered formalin (4 % formaldehyde) and examined under fluorescence microscopes (Nikon eclipseTE300) and a Nikon microscope (Nikon DXM1200F) with camera. The reagent wheat-germ agglutinin (FITC-WGA), which is found in organism structures like fungi walls, was used for dying MPs (Monsigni et al. 1979).

3. Results and discussion

3.1 Environmental variables

It has been demonstrated that the sorption behavior of MPs in the water column mainly depends upon the physicochemical variables (e.g., pH, temperature, DOM, and salinity), the nature and intrinsic properties of polymers as well as the presence of pollutants such as heavy metals and organic contaminants, among others (Tang et al. 2020; Binda et al. 2021; Forero-López et al. 2022). In this way, **Figure S2** ***(Supl. Material)*** shows how the temporal distribution of pH, salinity, DO, SPM, TPC, TPN, SPR, turbidity, Chl-*a*, and *phae*, during the assay in CP at the BBE, influence MPs sorption as well as the plastisphere development. The ranges of water temperature, pH, DO, and salinity were: 23.5 °C (in January, southern summer)–11.4 °C (in June, southern autumn), 6.8–8.3 (mean: 7.52, S.D.: 0.51), 7–8.9 $mg.L^{-1}$ (mean: 7.81 $mg.L^{-1}$, S.D.: 0.63), and 28.86-44.2 (mean: 36.13, S. D.: 5.22), respectively. Chl-*a* and *phae* varied between 9.61 and 0.32 $\mu g.L^{-1}$ (mean: 4.48, S.D.: 2.98 $\mu g.L^{-1}$) and 4.84 and 0.11 $\mu g.L^{-1}$ (mean: 0.95, S.D.: 1.60 $\mu g.L^{-1}$). In particular, Chl-*a*, and SPM, *phae*, and TPN were strongly associated throughout the assay. This was supported by the positive correlations detected between Chl-*a* and SPM ($r = 0.83$, $p = 0.01$, $N= 8$), Chl-*a* and *phae* ($r = 0.63$, $p = 0.09$, $N= 8$), and Chl-*a* and TPN ($r = 0.89$, $p = 0.007$, $N= 8$) (**Figure 2**). The physicochemical variables recorded during the assay (summer-autumn

period) are consistent with the historical values previously reported for the study zone (Spetter, 2006). Chl-*a* and phaeopigment values are related to the phytoplankton summer bloom with the highest Chl-*a* level in January (9.61 $mg.L^{-1}$). Such values are associated with planktonic and pennate diatoms as *Thalassiosira curviseriata, T. minima, T. pacifica, Thalassiosra hendeyi, Cyclotella striata, Chaetoceros* spp, and phytoflagellates (Guinder et al. 2013 and 2015; Spetter et al. 2015, Forero lopez et al. 2021b) (see **Figure S3**).

On the other hand, SPM, TPC, and turbidity ranges were 144.2-34.88 $mg.L^{-1}$ (mean: 73.36, S.D.: 40.50 $mg.L^{-1}$), 1.64-6.47 $mg.L^{-1}$ (mean: 3.26 $mg.L^{-1}$, S.D.:1.57), and 82-17 NTU (mean: 37.45, S.D.: 40.50 $mg.L^{-1}$), respectively. Also, SPM showed a positive correlation with TPN ($r = 0.87$, $p = 0.01$, $N = 8$), suggesting that SPM and Chl-*a* could be the main sources of organic and inorganic nitrogen. In particular, the high concentrations of SPM in CP are likely due to usual strong winds that promote resuspension and deposition of SPM, generating the high turbidity that characterizes the waters of this estuary (Cuadrado et al. 2005). During the assay, the composition of SPM was based on seston, minerals (quartz, feldspar, calcite, and clay), diatoms frustules, detritus, and silt sediments. Finally, the range of concentration of SPR varied from 1.62 to 3.75 μM (2.72 μM, S.D.: 0.63) while the range of concentration of TPN was 0.07 and 0.32 (0.16 $mg.L^{-1}$, S.D.: 0.09). SRP exhibited the lowest level at the beginning of the assay, coincident with the higher Chl-*a* value due to the uptake by the phytoplankton (Spetter et al. 2015; Forero-López et al. 2021a).

Theoretically, DOM substances present in the water column tend to form a conditioning film on MPs surface, changing their hydrophobicity, allowing the adhesion of microorganisms present in the water column and the generation of biofilm (Amaral-Zettler et al. 2020). In this way, the characterization of DOM through the fluorescence properties and

DOM composition are presented in **Figure S2** and **Table S2** ***(Supl. Material).*** The fluorophores $FDOM_C$, $FDOM_T$, $FDOM_{B,}$ and $FDOM_M$ were detected during the assay. $FDOM_M$ is associated with humic substances of low aromaticity and exhibit range from 2.45 to 3.66 (mean: 2.80, S.D.: 0.41). $FDOM_C$ exhibited ranges between 1.87 and 2.47 (mean: 2.14, S.D.: 0.21); these aromatic humic substances and recalcitrants come from the contribution of terrigenous humic material. On the other hand, the protein-like band components such as tryptophan or tyrosine aminoacid residuals ($FDOM_{B,T}$) (Wang et al. 2015) were also detected. $FDOM_B$ exhibited a range from 0.713 to 6.62 (mean: 2.53, S.D.: 2.32), while $FDOM_T$ showed values between 0.38 and 6.34 (mean: 2.95, S.D.: 1.77)**.** Both DOM components exhibited the higher values in April due to rainfall during this month (80 mm). BIX showed a strong correlation with $FDOM_T$ ($r = 0.91$, $p = 0.001$, $N = 8$) and with $FDOM_M$ ($r = 0.83$, $p = 0.01$, $N = 8$), indicating that they are related to biological and bacterial production. The distribution of the three fluorescence indices (HIX, BIX, and FIX) was also analyzed during the assay in CP (***Table S2, Supl. Material***). The humification index (HIX) and the biological index (BIX) exhibited ranges between 0.58 and 3.8 (mean: 1.82, S.D.: 0.97), and 0.88 and 2.89 (mean: 1.40, S.D.: 0.64), respectively. The higher values of HIX and BIX in CP during assay suggested a high degree of DOM humification, mainly derived from bacterial activity and other biological organisms classified as autochthonous sources (Huguet et al. 2009; Garzón-Cardona et al. 2021). The fluorescence index (FIX) ranged between 1.69 and 1.90 (mean: 1.73, S.D.: 0.07), indicating a predominance of the biogenic character to the bulk DOM pool. It is important to mention that pH, ionic strength, and Fe concentration can affect DOM fluorescence, while the humic substances of the bulk DOM pool tend to flocculate with increasing salinity (Huguet et al. 2009). Finally, FIX showed a positive correlation with SPM ($r = 0.77$, $p = 0.02$, $N = 8$) and with TPC ($r = 0.89$, $p = 0.007$,

N = 8), indicating that part of suspended matter comes from a biogenic source. In this way, the substances that composed the DOM may be humic and protein characters derived from bacterial activity and other autochthonous biological organisms in the assay zone.

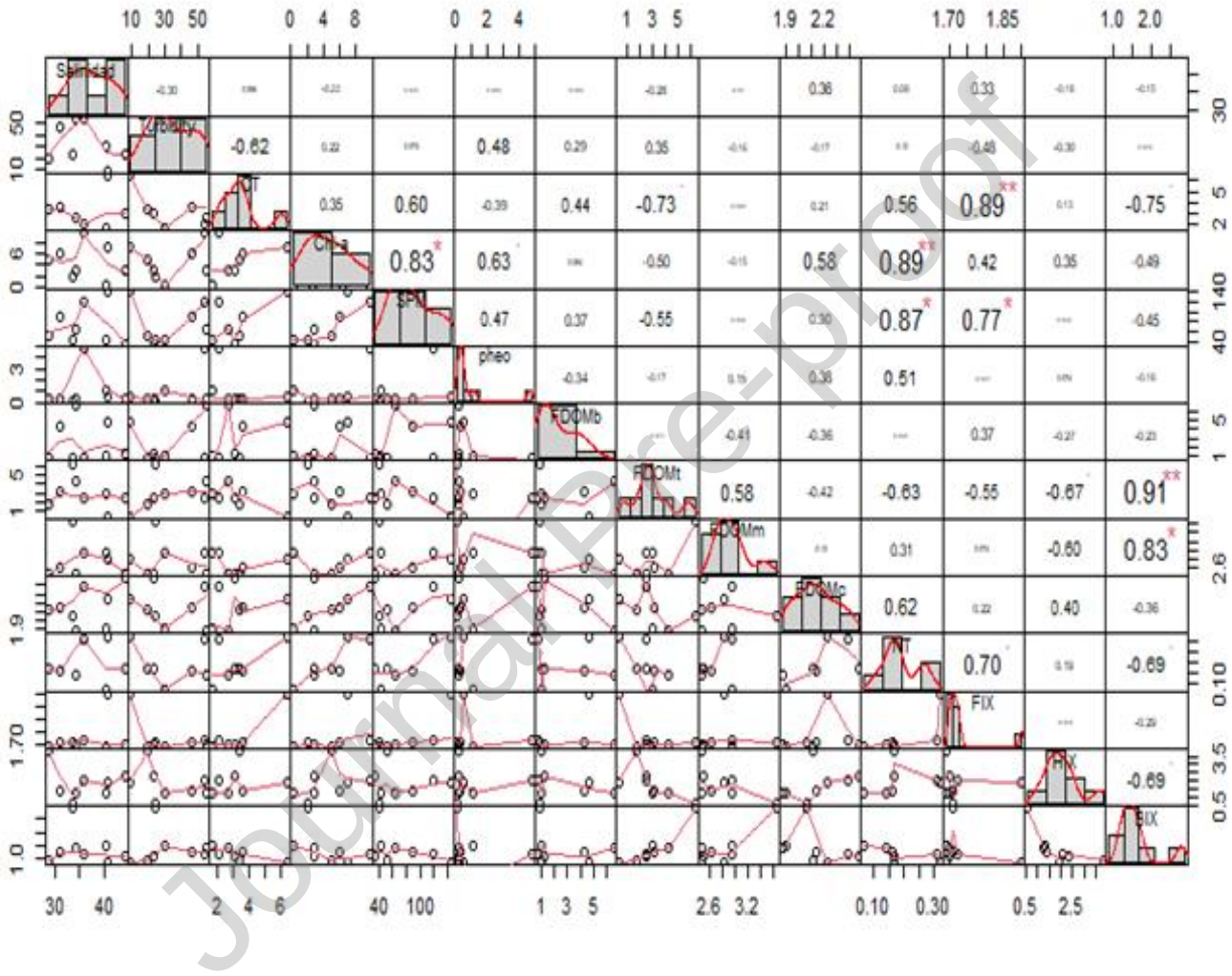

Figure 2. Correlation matrix (r values) between the physico-chemical variables (salinity, turbidity (NTU), TPN ($mg.L^{-1}$), chl-*a* and *phae* ($\mu g.L^{-1}$), TPC ($mg.L^{-1}$), SPM ($mg.L^{-1}$), fluorophores DOM ($FDOM_C$, $FDOM_T$, $FDOM_B$, and FDOM) and fluorescence indices (BIX, FIX, and HIX)),correlation graphics and Normal Probability Plots (Q-Q plots): *significant correlation. ** highly significant correlation.

3.2 Microbiology

The number of culturable heterotrophic bacteria on the submerged plastic increased during the experiment from 4.5 x 10^4 Colony Forming Units (CFU).cm^{-2} on day 14 to 8.0 x 10^4 CFU.cm^{-2} on day 129, and fluorescent *Pseudomonas* count was between 10 to 3.0 x 10^2 CFU.g^{-1}. Total coliform count ranged from 2.0 × 10^2 and 7.0 x 10^3 CFU.g^{-1} and *E. coli* was detected in all samples. The values of culturable vibrios ranged from 20 to 100 UFC.g^{-1}. A significant difference in the counts of filamentous fungi (Ascomycota) and yeasts was observed. Along the experiment, filamentous fungi counts ranged from 30 to 3.3 x 10^2 CFU.g^{-1}, during the first 56 days. After this time, two species of yeast (*Rhodotorula mucilaginosa* and *Candida tropicalis*) colonized MPs surfaces reaching mean values of 4 x 10^5 and 1.4 x 10^4 CFU.g^{-1}, respectively, until the last sampling time (129 days). There were no significant differences for microbial counts among NyMPs and PSMPs. In particular, the observation of fungi cultures revealed that all of them belonged to Ascomycota, and different genera like *Phona* s.l., *Alternaria* sp., *Penicillium* sp. and *Cladosporium* sp. formed aggregates in both types of MPs (**Figure 3**).

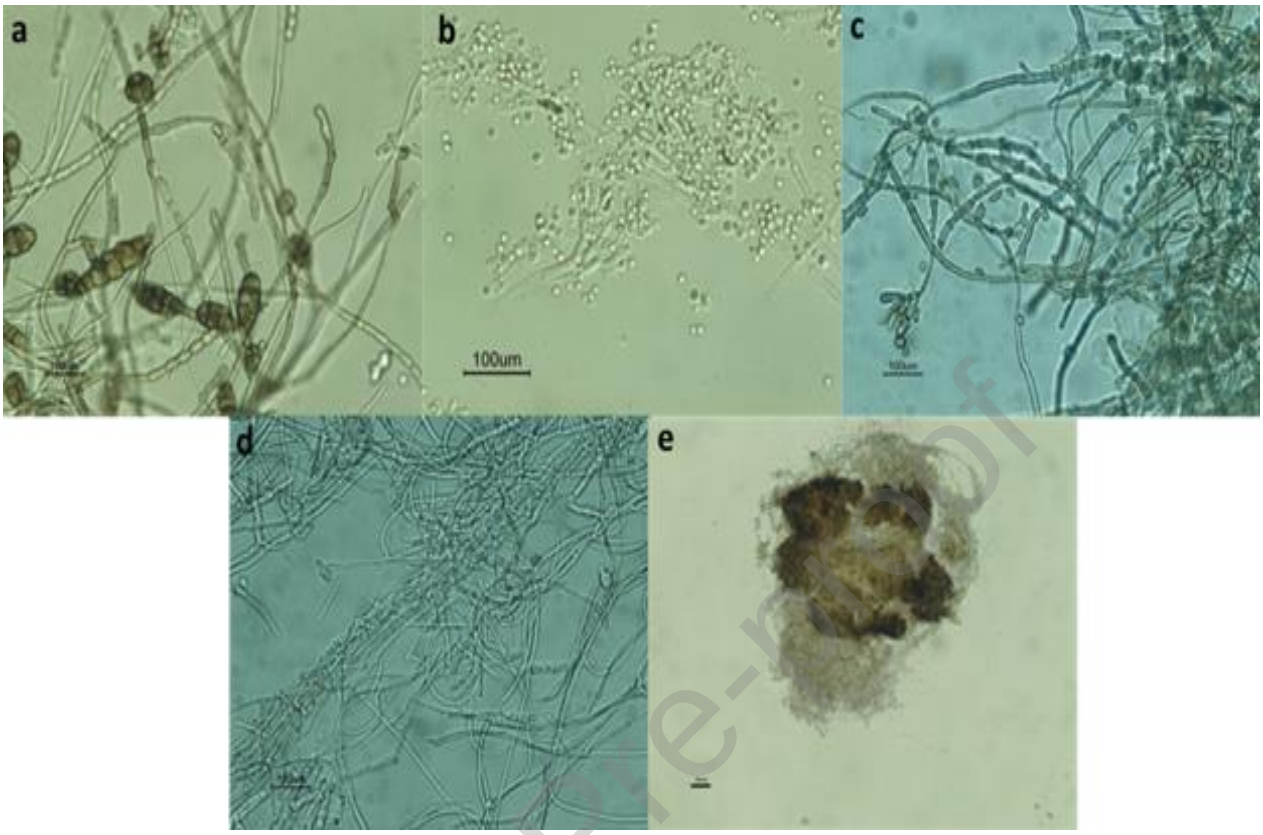

Figure 3. Photomicrographs of the fungi *Alternaria sp*. (a-100x), *Penicillium sp.* (b-40x), *Cladosporium sp.* (c-40x) and *Phona* s.l. (d-40x, e-10x) found on the MPs surface during the immersion assay in the inner zone of Cuatreros Port (CP), at the BBE.

It is evident that different taxonomic groups colonized MPs throughout the assay being heterotrophic bacteria, the first colonizers and the most abundant group of the plastisphere. Our results are similar to the results reported by other authors (e.g., Arias-Andrés, 2018; Pazos, et al. 2020). Besides, Arias-Andrés (2018) found that MP biofilms consistently differed from those in the surrounding water, demonstrating microorganisms diversity and abundance changes in the presence of MPs. Moreover, the same authors concluded that different environments lead to substantial changes in the biomass build-up and heterotrophic activities of MP biofilms. On the other hand, fungi found in the present study have also been described in previous studies of MPs colonization (Kettner et al. 2017).

However, to our knowledge few studies analyzed fungal diversity in natural waters associated with MPs. Most of them are focused on terrestrial ecosystems.

Bacterial adhesion is a highly controlled and regulated process by which adhering cells produce extracellular biopolymers to form structured and complex matrices (Costerton et al. 1995). Microbial biofilms can subsequently trigger the attachment of specific invertebrates and algae, which increases the degree of biofouling (Zardus et al. 2008). The prokaryotic and eukaryotic groups that live in plastic biofilms can also include potential pathogenic (Kirstein et al. 2016; Amaral-Zettler et al. 2020) or hydrocarbon-degrading organisms (Delacuvellerie et al. 2019; Oberbeckmann & Labrenz, 2020; Zhang et al. 2021).

MPs tend to facilitate the survival of faecal indicator organisms (e.g., *E. coli*) and human microbial pathogens (e.g., *Vibrio* and *Pseudomonas* genera) as base substrates, therefore, increasing human exposure routes by providing a vehicle for dispersal. It is evident that this area of marine environmental pollution research needs urgent investigation. The genus *Vibrio* is perceived as an opportunistic biofilm-former under appropriate growth conditions (Oberbeckmann et al. 2018; Xu et al. 2019). Other putative pathogens can be found selectively enriched on MPs such as *E. coli* and species belonging to *Pseudomonas* genus (Curren & Leong, 2019; Rodrigues et al. 2019; Silva et al. 2019; Wu et al. 2019). *Vibrio* spp. are ubiquitous in the marine environment, and its presence in MPs in this study suggests they may be part of the autochthonous biofilm community on most plastics found in coastal and estuarine regions. Whilst the culture-dependent methods used here do not differentiate *Vibrio* spp. types, potentially pathogenic species such as *V. cholerae, V. vulnificus* or *V. parahaemolyticus* have been previously isolated from plastic debris in coastal and estuarine regions of the North Sea (Kirstein et al. 2016).

3.3 SEM/EDX analysis in the plastisphere on MPs

SEM images of biofilm morphology and microbial colonization (e.g., bacteria, fungi, diatoms) on MPs surface exposed at different times of immersion are presented in **Figure 4**. As shown in **Figure 4 (a-b)**, no microbial community was found on NyMPs and PSMPs surfaces on day 0 of immersion. In general, microbial communities were present on MPs surface of the experimental group while none could be observed in the control group. In addition, a thick layer of exo-polymeric substances (EPSs) was observed on PSMPs, covering the surface, while on NyMPs, the distribution pattern was granular. However, both biofilms formed on MPs had some smooth and clean surface areas. A very dense microbial community surrounded and covered by EPSs could be observed on PSMPs surface on day 42 **Figure 4 (e-f),** a great number of cocci (green circles) and rod-shaped (red circles) bacteria according to morphology, yeast aggregates (blue circles), and fungal filaments (white arrows) can be seen. **Figure 4 (m-n)** exhibits the surface of PSMPs submerged during 129 days, which was almost covered by microbial communities (rod and cocci-shaped bacteria, yeast's microcolonies, and fungal filaments). **Figure 4 (h-k)** revealed that NyMPs present microcracks and pits (increased in surface roughness) and particles attached to their surface. As seen in **Figure 4 (c,d-g,h-k,l**) for NyMPs surface biofilm, agglomerated microorganisms were observed. They were covered with EPSs residues as well as cocci, and yeast aggregates. Aging defects on the NyMPs surface appeared after 42 (6 weeks) and 129 days (18.5 weeks) of immersion and could likely be attributed to the estuarine water flow fluctuation and UV effects (Cheng et al. 2021). Moreover, the magnitude of the forces generated on the MPs surface by the fluid flow depends on the water flow fluctuation and the shape and topography of the material polymer. These results agree with the reports of Cheng et al. (2021), where PP-thin-film MPs presented cracks after 5 weeks of immersion in estuarine waters. In the

case of PSMPs, as previously mentioned, due to their topography and great quantity of biomass and inorganic particles it was difficult to observe some type of degradation on the surface by SEM. In the qualitative observation of both type of MPs, other groups of organisms were also identified: filamentous fungi (Ascomycota-fungal structures: Zoospores and hyphae), diatoms, radiolarians dinoflagellata, and nematode (**Figure. S3, *Supl. Material***). From this analysis and SEM images (**Figure 3**), certain differences between PSMPs and NyMPs were observed. Both types of MPs were made up of particle aggregates (organic and inorganic) forming conglomerates associated/adhered to it where the organisms inhabit. This kind of structure was more noticeable in the PSMPs in the first 14 days, while on NyMPs was noticed 129 days later (***Figure 3*** and ***Figure S3 Supl. Material***). Moreover, the porosity of PSMPs provides a surface in which fungi could stick to it easier than the smooth and non-porous surface of NyMPs. Finally, Li et al. (2021b) reported that physicochemical variables (salinity, DOM, and pH) may be affecting the plastisphere bacterial community on the MPs surface. These same authors also informed the bacterial communities in the plastisphere on the MPs surface might be different and unique since MPs act as filters for microorganisms due to their hydrophobicity, high surface area, and the presence of some potentially hazardous polymeric additives in their structure (Li et al. 2021b).

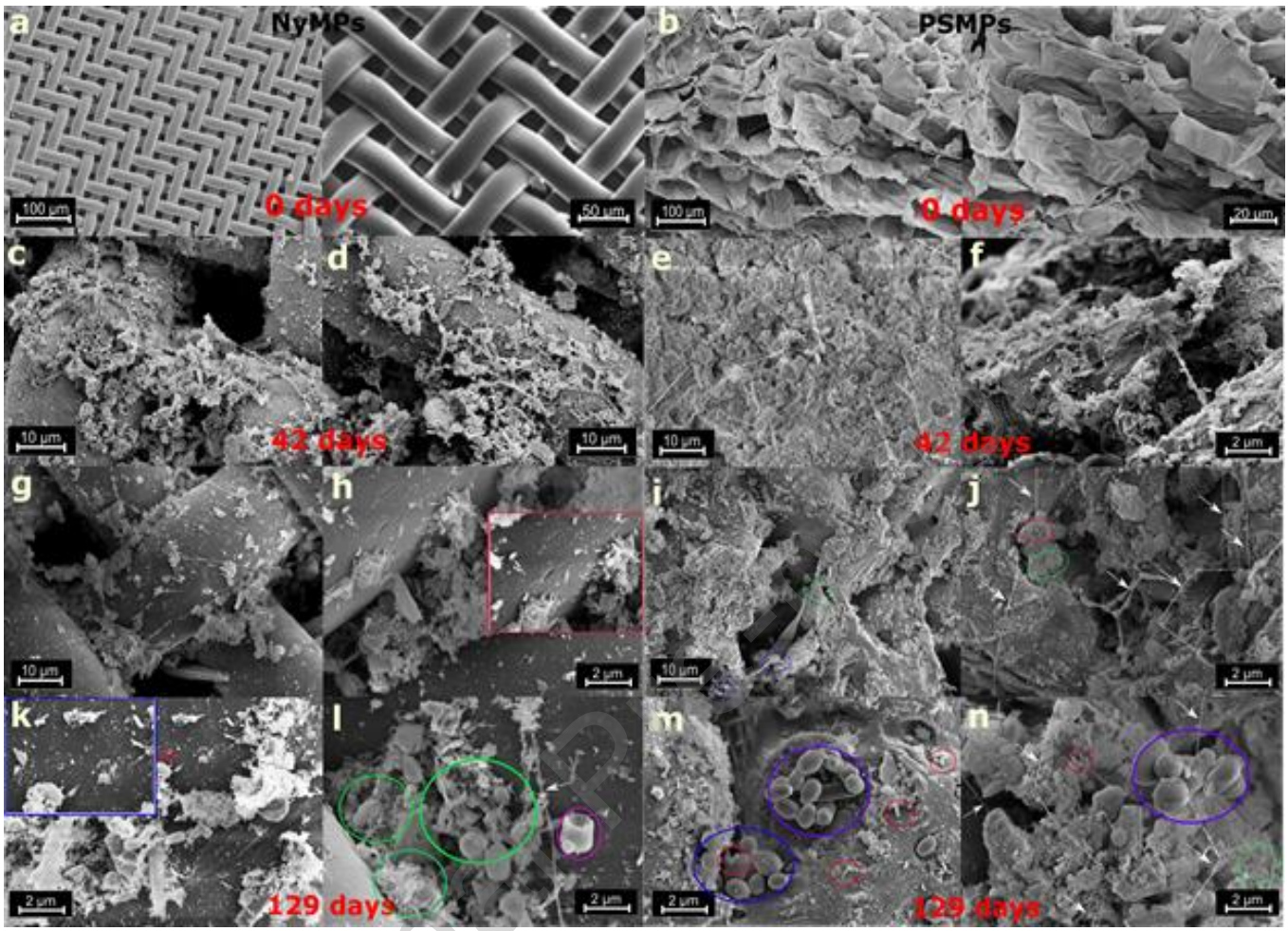

Figure 4. SEM images of the morphology of MPs: before the immersion at natural estuarine waters in the BBE: (a) NyMPs and (b) PSMPs. (c and d) NyMPs and (e and f) PSMPs exposed after 42 days of immersion. (g-h and k-l) NyMPs and (i-j and m-n) PSMPs exposed after 129 days of immersion.

The architecture of MPs could affect the texture and pattern of exopolymeric substances during the first stages of the formation of biofilms since the distribution pattern of EPSs on NyMPs surface was granular while PS was homogeneous. Moreover, each MPs type has different surface charges depending on the surface energy, hydrophobicity, and chemical composition (Oberbeckmann et al. 2014; Xie et al. 2021). In this way, De la Torre

et al. (2022) suggested that the architecture type of microscopy meshing of face masks could influence the growth of some microorganism communities as in the topography or texture of the biofilm. MPs not only provide a substrate to attach and proliferate, but also harbor several microplastic-degrading organisms. Several lines of evidence support this. Firstly, Reisser et al. (2014) noticed a variety of plastic surface microtextures, including pits and grooves, conforming the shape of several bacterial, fungal, and eukaryotic colonizers, revealing that these epiplastic communities are pivotal in plastic degradation. Secondly, several plastic-degrading bacteria, fungal and algal have been generally retrieved from plastics and MPs (Oberbeckmann et al. 2015a).

3.4 Chemical characterization of MPs

In this study, MPs were characterized before, during, and after the assay (**Figure 5).** The results showed that PSMPs have a rough hydrophobic surface and larger surface area than NyMPs. Due to their porosity and roughness they can affect the spheric form of water drops during the measurement of contact angle, increasing the measured value (Mahltig, 2016). According to the measurements, the contact angles of the MPs at 0 days of immersion were 107.2 ± 0.3 θ for PSMPs and 46.5 ± 0.1 θ for NyMPs. This result is a consequence of an increased surface energy due to polymer hydrophobicity. NyMPs exhibit a lower contact angle with decreased surface energy, indicating that their surface is hydrophilic (Lee, 2011). The results are according to the chemical structure of each polymer, where PS exhibits hydrophobic phenyl pending groups, while Ny has hydrophilic amide groups. After 42 days of immersion, the values of contact angles dropped considerably from 107.2 to 47.6 ± 0.1 θ and 46.5 to 24.3 ± 0.2 θ for PSMPs and NyMPs, respectively. Finally, after 129 days, the values of contact angles had a slight increase from 47.6 to 49.5 ± 0.3 θ for PSMPs and 24.3

to 30.1 ± 0.1 θ for NyMPs (**Figure 5a**). The hydrophobicity of MPs in the present study, decreased with the exposure time due to the adherence of organic and inorganic substances which formed a conditioning film (eco-corona) onto MPs surfaces and also a biofilm consistent with the report provided by Jin et al. (2020) and Cheng et al. (2021).

Figure 5a shows the variation percentage of MPs weight during the assay. Both types of MPs showed an increase in their weight during the assay, except at 70 days of immersion perhaps due to the maturing of the biofilm and/or its detachment from the surface of MPs. The biofilm formation influenced the electrostatic forces (repulsion) of plastic particles presenting lower repulsion during the time of immersion, consequently forming agglomerates of MPs interacting by biofilm. The increase in MPs weight during the assay was caused by attached biomass and minerals adhered to biofilm generated by microorganisms, changing the buoyancy and hydrophobicity of these plastic particles. After 129 days of immersion, the mass of both MPs had a significant increase of more than 100 % of their weight. Visually, after cleaning them and eliminating biofilm and particles adhered to their surface by ultrasonic treatment, it was observed that only NyMPs exhibited a change from white to a slightly yellowish color after the assay.

On the other hand, XRD diffractograms showed changes in the XRD patterns of the NyMPs before and after water immersion during 42 and 129 days (**Figure 5b1**). NyMPs pattern exhibited two sharp diffraction peaks characteristics at 20.5° and 23°, suggesting the presence of ∝ phase in the polymeric structure (Kayaci et al. 2012); Ny is a highly crystalline degree polymer because of the strong intermolecular hydrogen bonds that hold chains together forming crystalline regions. In contrast, PSMPs exhibited two wide peaks at 8° and between 17 and 37° corresponding to the diffraction generated by the distance between the

aromatic lateral rings and principal chains. The poor definition of the peaks indicated PS had roughly an amorphous structure (Gowd et al. 2002). According to the XRD diffractograms, the intensity in the signal of the crystal phase of NyMPs decreased with the time of immersion while the PSMPs did not exhibit a change in their structure during the experiment (**Figure 5b2)**. In addition, the diffractograms of PSMPs immersed at different times also exhibited characteristic peaks of quartz, albite, illite, halite, and other minerals, which are part of SPM. The characteristic signals that come from minerals that composite SPM may be due to these particles being embedded in the pores and roughness of PSMPs, indicating they were not completely eliminated during the cleaning of MPs. The mineralogical composition of SPM is consistent with that reported in a previous work where we studied the interactions between metal ions, SPM, and MPs in the same zone of study (Cuatreros Port) (Forero-López et al. 2021a). Some authors also found that crystallinity plays a governing role in the sorption process of some pollutants like dibutyl phthalate, which is used as polymeric additive (Yao et al. 2021), and organic contaminants (OC) (Fu et al. 2021). The diffraction peaks in the XRD pattern of NyMPs were less sharp after immersion for 129 days showing the beginning of crystallinity changes in accordance with the reports by Sudhakar et al. (2007) and Tang et al. (2020). Other researchers have reported that aged PSMPs present an increased crystallinity under seawater after being exposed to UV-light (Mao et al. 2020). However, in our study, PSMPs did not exhibit this behavior.

NyMPs TGA thermograms before and after the assay showed changes in the curves from two to three steps of successive polymer degradation after immersion, indicating the influence of the time under water on the Ny thermal stability properties. In general, before immersion, NyMPs exhibited thermal degradation beginning at ≈ 426.23 °C, with a mass

loss of 85.80 % assigned to the decomposition of the main fraction of the polymeric moieties, whereas a loss of about 2.62 % may be assigned to carbon residual and is observed at roughly 463.41°C (Fazeli et. 2022). Both mass losses are clearly evidenced in the TGA curve included in **Figure 5c1**. After contact with the marine environment during 129 days, the mass loss in the NyMPs has not undergone significant variation with respect to the pristine Ny, however differences in the decomposition temperatures are highly noticeable. DTGA A decrease from 426.23 to 400.54 °C (first peak) and 463.41 to 451. 15 °C (second peak), respectively at 0 and 129 days of immersion. This behavior may be associated with the erosion and deterioration of the MPs structure mediated by the environment conditions as well as by the presence of different organic /inorganic compounds that may function as catalysts of the thermal decomposition processes (Debroy et al. 2021) (**Figure 5c1**). TGA/DTGA profiles of PSMPs at 0 and 129 days of immersion are shown in **Figure 5c2**. DTGA thermograms of PSMPs exhibited a single step decomposition. After the assay, the curve showed a range of temperature between 330 °C to 465 °C with a polymer decomposition temperature at about 413.05 °C, where approximately 92% of weight loss of the sample takes place, which is in accordance with the existent literature (Dümichen et al. 2017). After aged in marine estuarine water during 129 days, PSMPs exhibited notable differences in both its TGA curve as well as in the decomposition temperature. This last increased from 413.05 °C to 425.12 °C, suggesting that the aged process provided thermal stability to PSMPs. Concerning the mass loss it is evident that only roughly 55% of mass is lost in the range of temperature evaluated. It is important to highlight that MPs were cleaned with distilled water and sonicated previous their characterization. Therefore, In the case of PSMPs, some SPM residuals, mainly composed of inorganic moieties, were trapped/caught in the porous structure of these plastic particles, changing the profile of the thermogram

curve and altering the decomposition temperature and weight loss percentage of MPs (Mansa and Zou, 2021).

Figure 5d shows the infrared spectra of Ny and PSMPs at 0, 42, and 129 days of immersion. In general, the ATR-FTIR spectra displayed typically representative bands of functional groups of Nylon 6,6 (**Figure 5d1**) and PS (**Figure 5d2**). In the case of NyMPs spectrum, bands at 3299, 1637 and 1560 cm^{-1} are found and related to the N-H amide I, and amide II stretching vibrations of the amide bond, respectively(Pretsch et al. 2009; Li et al. 2016). On the other hand, the PSMPs spectrum is characterized by the vibration modes of the phenyl groups, such as C-H aromatic stretching at 3038 cm^{-1}, and the typical aromatic overtones between 2000 and 1665 cm^{-1}. (Pretsch et al. 2009). The signals between 1400 and 1500 cm^{-1} are also associated with C=C stretching monosubstituted aromatic and C=C stretching vibrations in the aromatic ring, while the signal at 760 cm^{-1} is associated with the out-of-plane C-H bending vibrations of aromatic ring (Lian and Krimm, 1958; Pretsch et al. 2009). There are no substantial differences in the presence of functional groups of each type of MPs before and after immersion during 42 and 129 days. However, both MPs spectra present strong peaks at around 1045 cm^{-1}, which are attributed to inorganic PO_4^{3-} or NO^{3-} (Luna Zaragoza et al. 2009; Fu et al. 2021). However, some authors also have attributed stretching at ≈ 1048 cm^{-1} to Si–O, which is associated with clay minerals residuals (Suresh et al., 2017). PSMPs spectra recorded after aging during 42 and 129 days, present typical polymeric signals and those spectral signatures arising from residual biomass/biofilms (C=ONH from proteins, O–H from polysaccharides) on their surface located between 3400-3600 cm^{-1}.The results of FTIR analysis are consistent with those reported by Fu et al. (2021) and Salt et al. (2021). In particular, the last reported that organic matter residuals may yield

a wide range of signals which overlap the polymer ones. This fact would not allow to clearly distinguish between the polymeric and the biomass/ biofilm functional groups present in aged MPs (Salt et al. 2021).

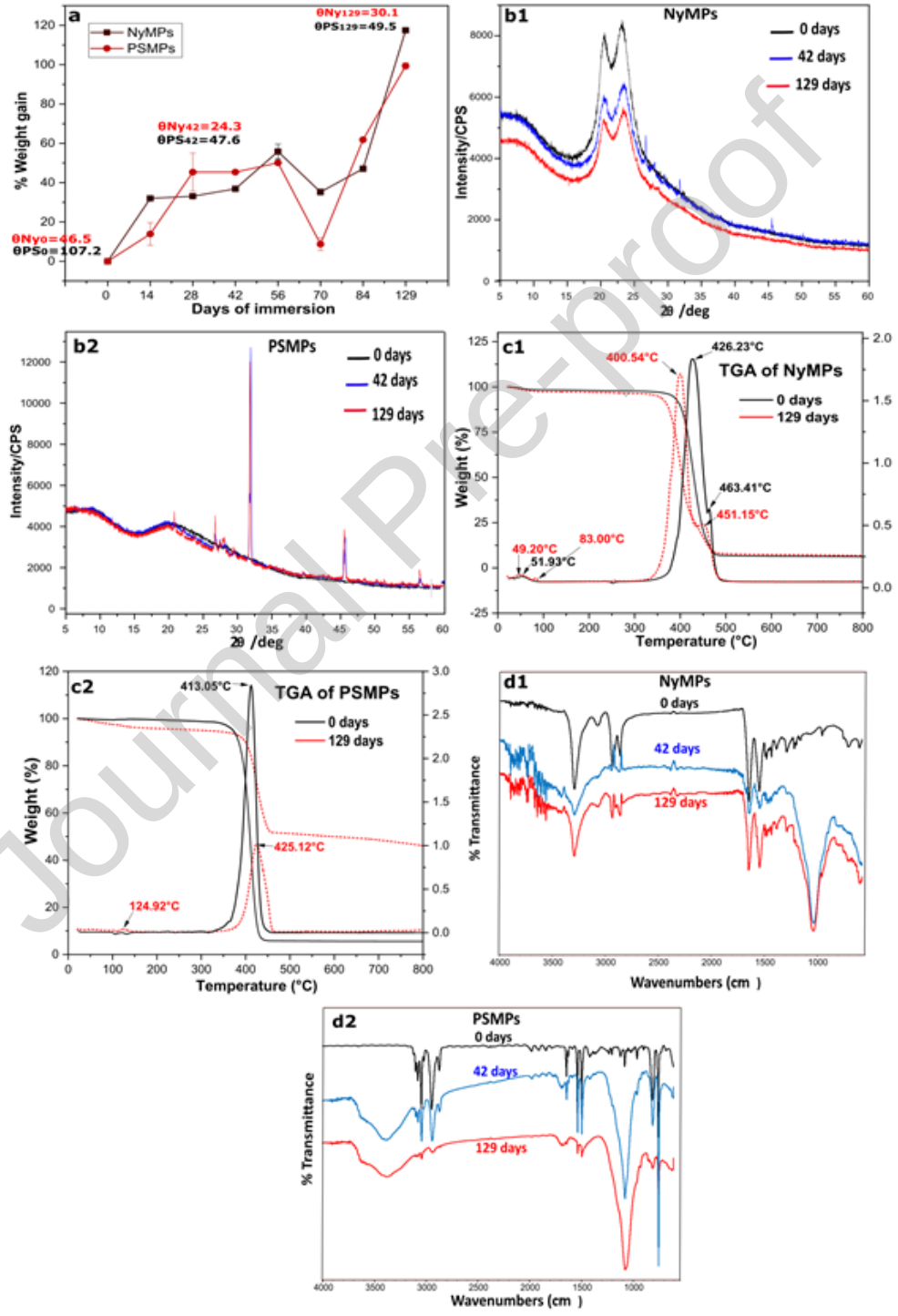

Figure 5. **(a)** variation of percentage of the NyMPs and PSMPs weight during the *in situ* experiment for 129 days in estuarine waters and their contact angle measurements at 0, 42, and 129 days of immersion. **(b)** XRD patterns of NyMPs and PSMPs at 0, 42, and 129 days of immersion. **(c)** TGA and DTGA curves of NyMPs and PSMPs before and after the assay and **(d)** ATR-FTIR spectra of NyMPs and PSMPs at 0, 42 and 129 days of immersion.

SEM images of MPs samples with their respective EDX spectrum at different times of immersion in the BBE waters are shown in **Figure 6.** SEM/EDX images of NyMPs and PSMPs at 0 days of immersion are presented in **Figures 6a-a1** where it can be appreciated that the elemental composition of NyMPs is C, O, and Ti, while PSMPs is composed by C. In particular, the peaks assigned to O besides the amide group, correspond to TiO_2 as well as Ti signal , which is widely used additive in the polymeric industry for instance as the white pigment (Cho and Choi, 2001). After 42 days of immersion, a significant quantity of EPSs, and suspended particulate matter (SPM) were observed on the surface of MPs (**Figure 6b-b1**). The EDX spectra of both types of MPs, after 42 days, exhibited strong C and O peaks followed by Al, Si, K, Mg, Ti, Fe, and Ca. EDX analysis (**Figure 6b**, spectrum) revealed the presence of peaks of Na on the NyMPs surface while Mo signals were only observed on PSMPs surface. Finally, SEM/EDX of MPs after 129 days immersion, (F**igure 6c-c1)** show small P peaks in both MPs types that could be associated with organic detritus and/or biofilm. Some authors have reported that biofilm formed on MPs surface could temporarily accumulate P and disturb the P cycle in the water because when biofilm matures, P is released (Chen et al. 2020). Moreover, in a previous work, we reported the presence of Mx-PO_3 (Mx: Ca, Mg, or Fe) and mixtures of Fe^{3+}/Fe^{2+} in the SPM of the water column of CP (Forero López et al. 2021a). Finally, a small peak of Mn was identified on NyMPs surface after 129 days of immersion. This metal presents historical high concentrations in SPM of the water column of the BBE (Fernandez-Severini et al. 2017 and 2018).

Some punctual EDX spectrum in NyMPs, before and after immersion, exhibited a change in the atomic percentage (At %) of Ti in the structure of MPs (see **Table S3).** Before the immersion, NyMPs showed an atomic percentage around ≈ 0.12% (S.D.: 0.03) of Ti. However, at 42 and 129 days of immersion the At % of Ti decreases to ≈ 0.05 (S.D.: 0.03) and ≈ 0.030% (S.D.: 0.03), respectively. These results may be indicating possible leaching of Ti from the NyMPs structure. However, the detection limit (LOD) in this technique depends on the sample surface conditions, thus, the smoother the surface leads to a lower LOD (Nasrazadani and Hassani, 2016). In this way, some authors have reported leaching of TiO_2 and $PbCrO_4$ pigments from MPs during their aging process in aquatic environments (Lou et al. 2019 and 2020). Moreover, these same authors also informed that the salinity could also

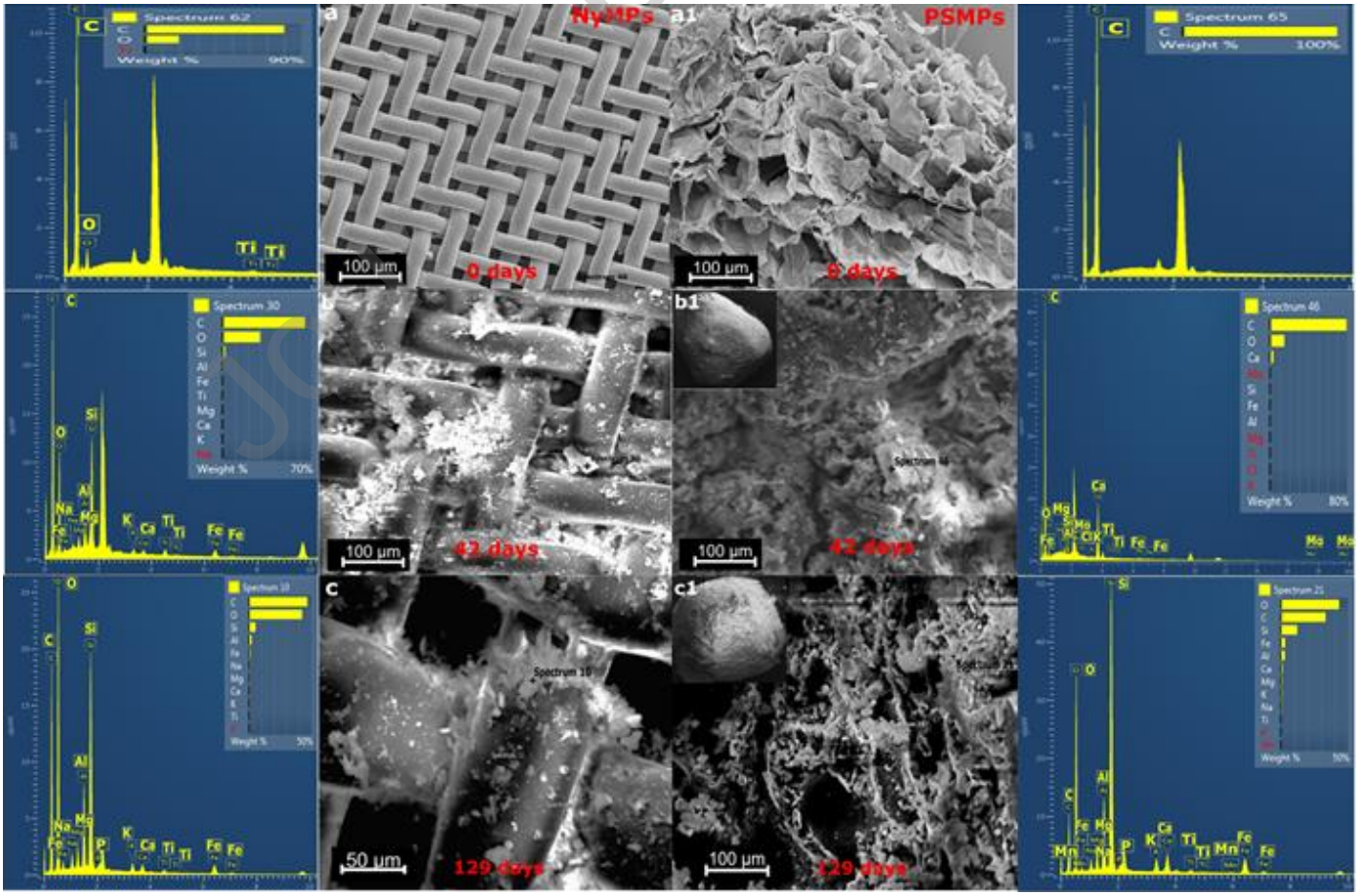

favor the leaching of these pigments from plastic particles.

Figure 6. SEM images of Ny and PSMPs with their respective EDX spectra at: (a) 0, (b) 42, and (c) 129 days of immersion in the BBE.

The use of a set of instrumental techniques for qualitative and quantitative analysis of MPs (e.g., FITR, XRD, SEM/EDX, and TGA) has been an indispensable component for studying the chemical, physical, and structural properties of these micromaterial pollutants and how the change of their properties can affect their sorption behavior in the environment (Tang et al. 2020 and 2021; Forero lopez et al., 2021a; Gao et al., 2021; Li et al. 2022; Wu et al., 2022; Sturm et al., 2022). Moreover, the principles on which each characterization technique is used have specific recommendations to prevent false positives or erroneous procedures during the characterization of material samples (Salt et al., 2021; Pizarro Ortega et al., 2022). Several chemical characterization techniques must be used together to obtain complete information about the nature of the material, such as their surface, structure, and composition. However, these techniques present some limitations to be used for chemical characterization on plastic pollution due to size range (meso/micro/nanoplastic), conductivity, structure (2D, or 3D), or surface contamination or impurities deposited in their structure, whose challenges and limitations have been evidenced in this work. As mentioned above, MPs surface contamination with biofilm or organic matter residue generated misassignment of functional group signals in FTIR spectra from MPs samples, and although these samples were cleaned three times by sonication for 20 min in our study, some biofilms residues remained in their 3D structure, affecting FTIR signals. Likewise, the presence of minerals or clay particles trapped in PSMPs structure modified the thermal decomposition and mass loss profile because the quantity and purity of the samples influence the shape of

the thermogram. In contrast, XRD analyses showed that the signals of mineral particles trapped in PSMPs structure did not affect the interpretation of XRD patterns over MPs crystallinity. However, for NyMPs, TGA technique was useful in our study to determine the humidity of NyMPs and leaching of additives (TiO_2) from the Ny matrix which also were evidenced through XRD patterns.

3.5. Heavy metals levels in the plastisphere on MPs

The concentrations of heavy metals (Cr, Mn, Cu, Zn, Cd, and Pb) were analyzed in the plastisphere on MPs surface during the assay. It is well known that MPs are vectors for the transport and reservoir of heavy metals in the aquatic environment (Turner and Holmes, 2015; Wang et al. 2017; Binda et al. 2021; Liu et al. 2022). The concentration levels of Cd and Mn in NyMPs ranged from <0.001 to 14.81 $\mu g.g^{-1}$d.w (mean: 6.38, S.D.: 5.77) and 80.53 to 885.6 $\mu g.g^{-1}$d.w. (mean: 295.6, S.D.: 269.09), whereas the concentration of these metals in PSMPs varied between 0.76 and 10.24 $\mu g.g^{-1}$ (mean: 5.60, S.D.: 2.84), and from 145.81 to 698.41 $\mu g.g^{-1}$ (mean: 326.10, S.D.: 181.52), respectively. Cu levels in Ny and PSMPs ranged from 1.68 to 255.97 $\mu g.g^{-1}$d.w., (mean: 44.15, S.D.: 93.78) and 1.30 to 22.97 $\mu g.g^{-1}$ d.w.(mean: 8.79, S.D.: 7.06), accordingly. On the other hand, the concentration levels of Cr and Pb in NyMPs ranged between <0.03 and 1638.36 $\mu g.g^{-1}$d.w. (mean: 345.87, S.D.: 722.64), and <0.02 and 27.38 $\mu g.g^{-1}$ d.w. (mean: 17.10, S.D.: 11.16), whereas in PSMPs varied between <0.03 and 2403,63 $\mu g.g^{-1}$ d.w. (mean: 415.55, S.D.: 973.99), and <0.02 and 21.91 $\mu g.g^{-1}$ d.w. (mean: 8.58, S.D.: 6.97). Finally, the concentration levels of Zn in Ny and PSMPs ranged from 14.88 to 319.04 $\mu g.g^{-1}$ d.w. (mean: 80.25, S.D.:107.21) and 7.34 to 29.22 $\mu g.g^{-1}$ d.w. (mean: 24.41, S.D.:11.18). Thus, the studied concentration levels of heavy metals in each type of MPs during the assay followed this order: Cr > Mn > Zn > Cu > Pb

>Cd. The highest levels of heavy metals were exhibited in PSMPs (Cr and Mn) than NyMPs, and Ny showed higher levels of Cu, Zn, Cd, and Pb than PSMPs. Also, while most of the heavy metals levels increased gradually until 45 days of immersion (**Figure S3**), Cr and Mn concentrations were extremely high for each MPs at 129 days of immersion. **Table 1** presents the correlation between heavy metals analyzed in the plastisphere on Ny and PSMPs and some physicochemical variables. Some heavy metals such as Zn and Cu-NyMPs, and Pb in PSMPs exhibited positive correlation with TPC, and SPR while Mn, from each type of MPs, showed a strong negative correlation with Chl-*a*. This negative correlation between Mn and Chl-*a* may be associated with photosynthesis processes since Mn is uptaken by phytoplankton or aquatic microorganisms (Raven et al. 1999). The positive correlations between Cr, Mn, and Cd may indicate that these metals have a constant proportion between them in the plastisphere of each type of MPs. Likewise, these same heavy metals exhibited high positive correlations with the increase of weight of both types of MPs during the assay, indicating their relation with organic or inorganic particulate matter (SPM), plankton, and other organisms that are part of the plastisphere.

Table 1. Correlation analysis indicated that heavy metals of the plastisphere on Ny and PSMPs were significantly correlated with some of the physicochemical variables as SPR, Chl-*a*, and TPC in the water column of Cuatreros Port (CP).

-----Table 1----------

Some authors have reported eutrophic conditions and pollutants like heavy metals and MPs in the inner zone of the BBE due to urban-industrial discharges from cities and industries near the estuary, harbor activities, and maritime traffic (Bielsa et al. 2022;

Fernandez-Severini et al. 2019). In particular, Cr has been detected in paint sheets (as additive) and on microfibres (as part of the particulate matter adhered or metal ion adsorbed) in the BBE (Truchet et al. 2022b) and sandy beaches near this estuary (Truchet et al. 2021b). Moreover, Cr dynamic behavior in the water column has been strongly influenced by the phytoplankton biomass and organic carbon (Villagran et al. 2019; Forero López et al. 2021a and 2021b), and its levels (dissolved and particulate) have increased during the last few years. In particular, Mn and Fe (hydr)-oxides are involved in the oxidation-reduction process and they tend to absorb dissolved heavy metals such as Cr in the water column of this estuary (Villagran et al., 2019; Forero López et al. 2021a and 2021b). The main source of Cr is sewage effluents, discharged into the estuary, while the source of Cd is attributed to freshwater inputs that transport and discharge fertilizers and PO_4^{3-} from agrochemical activities in the region (Truchet et al. 2022a). These correlations between these metals have also been reported in SPM and microplankton (Fernández-Severini et al. 2017; Villagrán et al. 2019). Some Cr and Cd levels, detected in both types of MPs, are extremely high in comparison with historical reports in SPM at CP, the BBE (**Table 2**) while values of other metals like Mn, Zn, and Pb are similar to historical data. In particular, Liu et al. (2021) found extremely high concentrations of Cd, Pb, and Zn in the plastisphere of microplastic samples from the waters surrounding Hong Kong. However, these authors indicated that SPM and plankton may be direct external sources of these metals in the plastisphere of MPs (Liu et al. 2021).

Table 2. Comparison of heavy metal levels found in the plastisphere on MPs in this study area and in other regions of the world ($\mu g.g^{-1}$). Historical level data of heavy metals in SPM and surface waters from the assay zone (CP). Data of abundance presented in ranges (minimum-maximum) and mean (± SD) of levels of heavy metals in the plastisphere on MPs.

-----Table 2----------

Although, it is widely reported both, pH and salinity strongly influence the sorption process between plastic particles and heavy metals (Tang et al. 2020 and 2021; Binda et al. 2021; Liu et al. 2022) no such relation has been detected in the present study. According to our results, the plastisphere on MPs surface is an important reservoir of heavy metals (in particular, Cr), as well as some pathogens such as *Vibrio* spp., *E. coli*, and *Pseudomonas* spp. In this sense, it is well known that microorganisms can bioaccumulate, biotransform, biomineralize, and extracellular precipitation of heavy metals in aquatic/terrestrial environments (Verma and Kuila, 2019). Metal-microbe interactions can occur through the mechanisms of metabolism-dependent bioaccumulation and metabolism-independent biosorption. The first mechanism is associated with the sequestration, redox reaction, and species-transformation methods (Igiri et al., 2018). In contrast, the second type comprises metal precipitation, adsorption, and chelation, which can occur on the surface of the microbes (Selenska-Pobell, and Merroun, M. 2010; Igiri et al., 2018; Verma and Kuila, 2019). In particular, the biosorption by surface interaction between microorganisms and heavy metals can occur mainly due to metal-binding with functional groups such as carboxyl and phosphate groups from different biopolymers that comprise cell walls of microorganisms (Selenska-Pobell, and Merroun, M. 2010; Verma and Kuila, 2019). The functional groups (carboxyl, amino, phosphate, and -OH) contained in the biofilm residuals were identified by ATR-FTIR. They tend to form complexes with metal ions (Guan et al. 2020) and these same complexation processes also tend to occur in SPM due to their organic and clayey composition. According to our previous works, surface hydroxyl groups of some minerals

contained in SPM clay fractions provide adsorption sites for dissolved metal cations and complexions in seawater (Forero-López et al. 2021a). In particular, the highest levels of heavy metals in the plastisphere on PSMPs may be due to their pore size, architecture (3D structure), and high surface area since they may contribute to greater retention of SPM, organic matter, and phytoplankton that contain heavy metals.

In a previous work, it was reported that the native phytoplankton from the study zone drives the Cr particulate dynamic as an efficient scavenger of Cr, as well as the redox processes between Fe and Mn species also affect the Cr speciation in the water column (Forero Lopez et al. 2021). As previously mentioned, the chelation between metal ions and extracellular polymeric substances (e.g., polysaccharides) from biofilm could also contribute to high levels of heavy metals in the plastisphere formed on MPs surface. However, this would not be the only mechanism that has been reported between biofilms and heavy metals, since immobilization and reduction of metal ions can also co-occur (Zhao et al. 2023). For example, Cr (VI) (dissolved Cr) can be reduced to Cr(III) by biofilm or can also be immobilized with phosphate on the biomass and the phytoplankton that comprises the biofilm (Wu et al. 2022; Zhao et al. 2023). In this way, Wu et al. (2022) reported that PS particles with the size of 4 mm covered with fungus biofilm had higher adsorption capacity towards Cu(II) and the ability to reduce Cr(VI) under lab conditions. Likewise, some authors have informed that bacteria such as *Pseudomonas spp* have the ability to reduce highly toxic Cr(VI) to less toxic Cr(III) and immobilize Cr(III) in the natural environment (An et al. 2020; Zhao et al. 2023). Moreover, the adsorption competition between dissolved Cr and other metals such as Cu or different types of pollutants present in the water column may affect the accumulation of Cr on the aged surface of MPs (Li et al. 2022; Zhou et al. 2022).

In particular, Li et al. (2022) reported that the presence of Cu may promote the adsorption of dissolved Cr on PE and PS more than on PA-MPs. Furthermore, these same authors also informed that the saturation adsorption of Cr(VI) depends of the physicochemical properties on MPs surfaces, their weathering degree and the interactions of types of Van der Waals forces (Li et al. 2022).

NyMPs have a hydrophilic surface because of amide groups in their chemical structure, leading to a better interaction between microorganisms than PSMPs, since its surface is hydrophobic (Sudhakar et al. 2007; Lee, 2011). Moreover, the colonization of microorganisms and biofilm growth on the MPs surface is one of the prerequisites prior to the degradation of plastic particles in the water column (Sudhakar et al. 2007). In this way, the first signs of weathering, such as surface damage (microcracks and pits) and a change of crystallinity were only observed in NyMPs, indicating an increased surface area as well as the beginning of some changes in the intrinsic properties of the material that can lead to MPs fragmentation over time. Moreover, the leaching of TiO_2 from the Ny polymeric matrix, could generate a change in their structure, leading to a decrease in the XRD signal intensity of NyMPs at 42 and 129 days of immersion. TGA thermograms evidenced a decrease in the onset decomposition temperature with decreasing polymer degradation time at 129 days maybe due to a reduction of crystallinity generated by a change in the polymer structure because of leaching of additives from MPs, indicating the first steps of weathering degradation. On the other hand, some authors have reported that some marine bacteria (e,g., Bacillus, Bacillus, and Brevundimonas) can degrade and decrease the crystallinity of the Ny 6.6, and 6 polymers in 3 months (Sudhakar et al. 2007). However, the effect of environmental stressors on MPs crystallinity has not been studied in depth and most

publications have focused on how the crystallinity change affects the microparticle sorption process. Nevertheless, according to Chen et al. (2020), salt content in seawater may promote the formation of β crystals in polypropylene (PP) microplastic, thus affecting its crystalline structure**.**

4. Conclusion

The present contribution comprised an unprecedented multidisciplinary approach to study weathering in two types of MPs (Ny and PS), and heavy metal accumulation in their plastisphere, formed during 129 days of immersion, in a polluted estuarine environment. During the assay, pathogenic microorganisms such as *Vibrio* spp., *Pseudomonas* spp. and *E. coli* abounded in both types of MPs that acted as dispersal vectors of these pathogens in moving estuarine waters.

Heavy metals such as Cr and Cd presented high levels of accumulation on the plastisphere surface of MPs, highlighting potential risks and threats to aquatic life. The topographic characteristics (architecture or 3D structure and porosity) and the surface area of PSMPs could be contributing to the highest retention or accumulation of heavy metals in the plastisphere in comparison with NyMPs. However, extensive characterization showed mechanical deterioration of the surface and decreased crystallinity in NyMPs due to water fluctuation and microorganisms, with implications for TiO_2 leaching from plastic particles, which represents a real threat with direct repercussions on the aquatic ecosystem. Therefore, future works should further investigate how heterotrophic microorganisms, phytoplankton, and SPM can increase the accumulation of heavy metals in the plastisphere and its chemical sorption behavior.

Declaration of competing interest

The authors declare that they have no known competing financial interests or personal relationships that could have appeared to influence the work reported in this paper.

Acknowledgments

We thank Prof. Madeleine Raño for correcting the manuscript in English language. Also, we thank Prof. Dr. María Virginia Bianchinotti for helping us with fungi taxonomy. This study was supported by PICT 2019-2241 (FONCYT, Argentina) granted to Dr. Melisa Fernández-Severini, and PGI UNS 24/Q109 granted to Dr. Carla Spetter.

References

Agustín, M.D.R., and Brugnoni, L. 2018. Multispecies biofilms between Listeria monocytogenes and Listeria innocua with resident microbiota isolated from apple juice processing equipment. *J Food Saf., 38,* e12499. doi:10.1111/jfs.12499

American Public Health Association (APHA), 1998. Standard Methods for the Examination of Water and Wastewater. American Public Health Association, Washington, D.C., APHA (680 pp.).

Amaral-Zettler, L.A., Zettler, E.R., and Mincer, T.J. 2020. Ecology of the plastisphere. *Nat. Rev. Microbiol.* 8, 139-151 doi:10.1038/s41579-019-0308-0

Amelia, T.S.M., Khalik, W.M.A.W.M., Ong, M.C. et al. 2021. Marine microplastics as vectors of major ocean pollutants and its hazards to the marine ecosystem and humans. *Prog Earth Planet Sci*, 8, 12. doi:10.1186/s40645-020-00405-4

An, Q., Deng, S., Xu, J., Nan, H., et al. 2020. Simultaneous reduction of nitrate and Cr (VI) by Pseudomonas aeruginosa strain G12 in wastewater. *Ecotoxicol Environ Saf., 191,* 110001. doi:10.1016/j.ecoenv.2019.110001

Arias-Andres M., Kettner M.T., Miki T., Grossart H.P. 2018. Microplastics: New substrates for heterotrophic activity contribute to altering organic matter cycles in aquatic ecosystems. *Sci. Total Environ.* 635: 1152-1159. doi:10.1016/j.scitotenv.2018.04.199

Bhagat, J., Nishimura, N., Shimada, Y. 2020. Toxicological interactions of microplastics/nanoplastics and environmental contaminants: Current Knowledge and Future Perspectives. *J. Hazard. Mater.,* 405, 123913. doi:10.1016/j.jhazmat.2020.123913

Bielsa, G.B., Berasategui, A.A., Dutto, M.S. et al. 2022. The effect of untreated sewage discharge in food availability, egg production, and female survival of the copepod Acartia tonsa in a southwestern Atlantic estuary. *Reg. Stud. Mar*, 49, 102139. doi:10.1016/j.rsma.2021.102139

Binda, G., Spanu, D., Monticelli, D., Pozzi, A., Bellasi, A. et al. 2021. Unfolding the interaction between microplastics and (trace) elements in water: A critical review. *Water Res.*, 204, 117637. doi: 10.1016/j.watres.2021.117637

Brennecke, D., Duarte, B., Paiva, F., Caçador, I., Canning-Clode, J. 2016. Microplastics as vector for heavy metal contamination from the marine environment. *Estuar. Coast. Shelf Sci.* 178, 189–195.doi:10.1016/j.ecss.2015.12.003

Carbone, M.E., Spetter, C.V., and Marcovecchio, J.E. 2016. Seasonal and spatial variability of macronutrients and Chlorophyll a based on GIS in the South American estuary (Bahía Blanca, Argentina). *Environ. Earth Sci.,* 75(9), 1-13.

Chen, Q., Wang, Q., Zhang, C., Zhang, J., Dong, Z., and Xu, Q. 2021. Aging simulation of thin-film plastics in different environments to examine the formation of microplastic. *Water Res.*, 202, 117462. doi:10.1016/j.watres.2021.117462

Chen, X., Chen, X., Zhao, Y., Zhou, H., Xiong, X., and Wu, C. 2020. Effects of microplastic biofilms on nutrient cycling in simulated freshwater systems. *Sci. Total Environ.* 719, 137276. doi:10.1016/j.scitotenv.2020.137276

Cho, S., and Choi, W. 2001. Solid-phase photocatalytic degradation of PVC–TiO2 polymer composites. Journal of Photochemistry and Photobiology A: *Chemistry*, 143(2-3), 221-228. doi:10.1016/S1010-6030(01)00499-3

Coble, P.G. 1996. Characterization of marine and terrestrial DOM in seawater using excitation-emission matrix spectroscopy. *Marine chem.*, 51(4), 325-346.

Cole, M., Lindeque, P., Fileman, E., Halsband, C., Galloway, T.S. 2015. The impact of polystyrene microplastics on feeding, function and fecundity in the marine copepod Calanus helgolandicus. *Environ Sci. Technol.,* 49, 1130–1137. doi:10.1021/es504525u.

Costerton, J.W., Lewandowski, Z., Caldwell, D.E., et al. 1995. Microbial biofilms. Annual review of microbiology, 49(1), 711-745.

Cuadrado, D.G.; Gomez, E.A., Ginsberg, S.S., 2005. Tidal and longshore sediment transport associated to a coastal structure. *Estuar. Coast. Shelf Sci.* 62(1), 291–300.

Curren, E., and Leong, S.C.Y. 2019. Profiles of bacterial assemblages from microplastics of tropical coastal environments. *Sci. Total Environ.* 655, 313-320. doi: 10.1016/j.scitotenv.2018.11.250

Debroy, A., George, N., and Mukherjee, G. 2021. Role of biofilms in the degradation of microplastics in aquatic environments. *J. Chem. Technol. Biotechnol.* doi:10.1002/jctb.6978

Delacuvellerie, A., Cyriaque, V., Gobert, S., Benali, S., Wattiez, R. 2019. The plastisphere in marine ecosystem hosts potential specific microbial degraders including Alcanivorax borkumensis as a key player for the low-density polyethylene degradation. *J. Hazard. Mater.*, 380, 120899. doi:10.1016/j.jhazmat.2019.120899

Deng, Y., Zhang, Y., Qiao, R., Bonilla, M.M., Yang, X., Ren, H., Lemos, B., 2018. Evidence that microplastics aggravate the toxicity of organophosphorus flame retardants in mice (Mus musculus). *J. Hazard. Mater.,* 357, 348-354. doi: 10.1016/j.jhazmat.2018.06.017.

Deng, H., Fu, Q., Li, D., Zhang, Y., et al., 2021. Microplastic-associated biofilm in an intensive mariculture pond: Temporal dynamics of microbial communities, extracellular polymeric substances and impacts on microplastics properties. *J. Clean. Prod.* 319, 128774. doi:10.1016/j.jclepro.2021.128774

De-la-Torre, G.E., Dioses-Salinas, D.C., Pizarro-Ortega, C.I., Fernández Severini, M.D., ForeroLópez, A.D., Mansilla, R., Ayala, F., Jimenez Castillo, L.M., et al. 2022. Binational survey of personal protective equipment (PPE) pollution driven by the COVID-19 pandemic in coastal environments: Abundance, distribution, and analytical characterization. *J. Hazard. Mater.* (2022) 426, 128070. doi:10.1016/j.jhazmat.2021.128070

Diaz-Jaramillo, M., Islas, M.S., Gonzales, M., 2021. Spatial distribution patterns and identification of microplastics on intertidal sediments from urban and semi-natural SW Atlantic estuaries. *Environm. Pollut.*,273, 116398. doi:10.1016/j.envpol.2020.116398

Dümichen, E., Eisentraut, P., Bannick, C.G., et al. 2017. Fast identification of microplastics in complex environmental samples by a thermal degradation method. *Chemosphere*, 174, 572-584. doi:10.1016/j.chemosphere.2017.02.010

Eberlein K y Kattner G (1987). Fresenius' Zeitschrift für analytische Chemie. Vol. 326, Issue 4: 354 - 357

Fazeli, M., Fazeli, F., Nuge, T. et al. (2022). Study on the Preparation and Properties of Polyamide/Chitosan Nanocomposite Fabricated by Electrospinning Method. *J Polym Environ*, 30, 644–652. doi:10.1007/s10924-021-02229-9

Federal Register. (1984). Definition and procedure for the determination of the method detection limit. Code of Federal Regulations, Part 136, Appendix B, October 26. *Federal Register*, *49*(209), 43430-43431.

Fernández Severini, M.D., Botté S.E., Hoffmeyer M.S., Marcovecchio, J. E. 2011. Lead Concentrations in Zooplankton, Water, and Particulate Matter of a Southwestern Atlantic Temperate Estuary (Argentina). *Arch. Environ. Contam. Toxicol.,* 61, 243 - 260. doi: 10.1007/s00244-010-9613-3

Fernández Severini, M.D., Carbone, M.E., Villagran, D.M., & Marcovecchio, J.E. 2018. Toxic metals in a highly urbanized industry-impacted estuary (Bahia Blanca Estuary, Argentina): spatio-temporal analysis based on GIS. *Environ. Earth Sci.* 77(10). doi:10.1007/s12665-018-7565-5

Fernández Severini, M.D., Villagran, D.M., Biancalana, F., Berasategui, A.A., et al. 2017. Heavy Metal Concentrations Found in Seston and Microplankton from an Impacted Temperate Shallow Estuary along the Southwestern Atlantic Ocean. *J. Coast. Res.* 335, 1196–1209. doi:10.2112/jcoastres-d-16-00151.1

Fernández Severini, M.D., Villagran, D.M., Buzzi, N.S., Chatelain Sartor, G. 2019. Microplastics in oysters (Crassostrea gigas) and water at the Bahía Blanca Estuary (Southwestern Atlantic): An emerging issue of global concern. *Reg. Stud. Mar. Sci*. 32, 100829- 100840. doi: 10.1016/j.rsma.2019.100829

Fernandez-Severini, M.D., Buzzi, N.S., Forero López, A.D. et al. 2020. Chemical composition and abundance of microplastics in the muscle of commercial shrimp *Pleoticus muelleri* at an impacted coastal environment (Southwestern Atlantic). *Mar. Pollut. Bull.* 161; 111700-11711. doi:10.1016/j.marpolbul.2020.111700.

Forero López, A.D., Truchet, D.M., Rimondino, G.N., Maisano, L., Spetter, C.V., et al. 2021a. Microplastics and suspended particles in a strongly impacted coastal environment: composition, abundance, surface texture, and interaction with metal ions. *Sci. Total Environ.* 754, 142143-142430. doi:10.1016/j.scitotenv.2020.142413.

Forero Lopez, A.D., Villagran, D.M., Fernandez, E.M., Buzzi, N.S., Spetter, C.V., Fernandez Severini, M.D. 2021b. Chromium behavior in a highly urbanized coastal area (Bahía Blanca estuary, Argentina). *Mar. Pollut. Bull.* 165, 112093. doi. org/10.1016/j.marpolbul.2021.112093.

Forero López, A.D., Fabiani, M., Lassalle, V.L., Spetter, C.V., Fernandez-Severini, M.D. 2022. Critical review of the characteristics, interactions, and toxicity of micro/nanomaterials pollutants in aquatic environments. *Mar. Pollut. Bull., 173276*. doi:10.1016/j.marpolbul.2021.113276

Forero López, A.D., Rimondino, G.N., Truchet, D.M., Colombo, C.V., et al. 2021c. Occurrence, distribution, and characterization of suspended microplastics in a highly impacted estuarine wetland in Argentina. *Sci. Total Environ.* 785, 147141. doi: 10.1016/j.scitotenv.2021.147141

Freije, R.H., Spetter, C.V., Marcovecchio, J.E., Popovich, C.A., Botté, S.E. et al. 2008. Water chemistry and nutrients in the Bahía Blanca estuary. In: Neves, R., Baretta, J. & Mateus, M. (Eds.), Perspectives on Integrated Coastal Zone Management in South America. IST Press, Lisbon, pp. 243–256.

Fu, L., Li, J., Wang, G., Luan, Y., Dai, W. 2021. Adsorption behavior of organic pollutants on microplastics. *Ecotoxicol. Environ. Saf.* 217, 112207. doi:10.1016/j.ecoenv.2021.112207

Gao, X., Hassan, I., Peng, Y., Huo, S., and Ling, L. 2021. Behaviors and influencing factors of the heavy metals adsorption onto microplastics: A review. *J. Clean. Prod., 319*, 128777.doi:10.1016/j.jclepro.2021.128777

Gao, L., Fu, D., Zhao, J., Wu, W., et al. 2021. Microplastics aged in various environmental media exhibited strong sorption to heavy metals in seawater. *Mar. Pollut. Bull., 169*, 112480. doi:10.1016/j.marpolbul.2021.112480

Garzón-Cardona, J.E., Guinder, V.A., Alonso, C., Martínez, A.M., et al. 2021. Chemically unidentified dissolved organic carbon: A pivotal piece for microbial activity in a productive area of the Northern Patagonian shelf. *Mar. Environ. Res.*, 167, 105286. doi:10.1016/j.marenvres.2021.1052

Gasperi, J., Wright, S.L., Dris, R., Collard, F., Mandin, C., et al. 2018. Microplastics in air: are we breathing it in?. Current Opinion in Environmental Science & Health, 1, 1-5.

Guinder, V. A., Popovich, C. A., Molinero, J. C., & Marcovecchio, J. 2013. Phytoplankton summer bloom dynamics in the Bahía Blanca Estuary in relation to changing environmental conditions. *Cont. Shelf Res.* 52, 150-158.

Guinder, V.A., López-Abbate, M.C., Berasategui, A.A., et al. 2015. Influence of the winter phytoplankton bloom on the settled material in a temperate shallow estuary. *Oceanologia* 57 (1), 50–60. doi:10.1016/j.oceano.2014.10.002

Guan, J., Qi, K., Wang, J., Wang, W., Wang, Z. et al. 2020. Microplastics as an emerging anthropogenic vector of trace metals in freshwater: Significance of biofilms and comparison with natural substrates. *Water Research, 184*, 116205.

Guo, J.-J., Huang, X.-P., Xiang, L., Wang, Y.-Z., et al. 2020. Source, migration and toxicology of microplastics in soil. *Environ. Int.* 137, 105263. doi:10.1016/j.envint.2019.105263

Gao, L., Fu, D., Zhao, J., Wu, W., Wang, Z. et al. 2021. Microplastics aged in various environmental media exhibited strong sorption to heavy metals in seawater. *Mar. Pollut. Bull.*, 169, 112480. doi:10.1016/j.marpolbul.2021.112480

Gowd, E.B., Nair, S.S., and Ramesh, C. 2002. Crystalline transitions of the clathrate (δ) form of syndiotactic polystyrene during heating: studies using high-temperature X-ray diffraction. Macromolecules, 35, 22, 8509–8514. doi:10.1021/ma020640h

Holm-Hansen, O., Lorenzen, C.J., Holmes, R.W., and Strickland, J.D. 1965. Fluorometric determination of chlorophyll. ICES Journal of Marine Science, 30(1), 3-15.

Horton, A.A., Walton, A., Spurgeon, D.J. et al. 2017. Microplastics in freshwater and terrestrial environments: evaluating the current understanding to identify the knowledge gaps and future research priorities. *Sci. Total Environ.*, 586, 127-141. doi:10.1016/j.scitotenv.2017.01.190

Huguet, A., Vacher, L., Relexans, S., Saubusse, S. et al. 2009. Properties of fluorescent dissolved organic matter in the Gironde Estuary. *Organic Geochemistry*, *40*(6), 706-719.

Igiri, B. E., Okoduwa, S. I., Idoko, G. O., Akabuogu, E. P., et al. (2018). Toxicity and bioremediation of heavy metals contaminated ecosystem from tannery wastewater: a review. *Journal of toxicology*. https://doi.org/10.1155/2018/2568038

Jin, M., Yu, X., Yao, Z., Tao, P., et al. 2020. How biofilms affect the uptake and fate of hydrophobic organic compounds (HOCs) in microplastic: Insights from an In situ study of Xiangshan Bay, China. Water Res. 184, 116118. doi:10.1016/j.watres.2020.116118.

Kalčíková, G., & Bundschuh, M. 2021. Aquatic Biofilms – Sink or Source of Microplastics? A Critical Reflection on Current Knowledge. *Environ. Toxicol. Chem.* doi:10.1002/etc.5195

Kayaci, F., Ozgit-Akgun, C., Donmez, I., Biyikli, N., & Uyar, T. 2012. Polymer–Inorganic Core–Shell Nanofibers by Electrospinning and Atomic Layer Deposition: Flexible Nylon–ZnO Core–Shell Nanofiber Mats and Their Photocatalytic Activity. ACS Applied Materials & Interfaces, 4, 6185–6194. doi:10.1021/am3017976

Kettner, M.T., Rojas-Jimenez, K., Oberbeckmann, S. et al. 2017. Microplastics alter composition of fungal communities in aquatic ecosystems. *Environ. Microbiol.* 19, 4447–4459. doi:10.1111/1462-2920.13891

Kirstein, I.V., Kirmizi, S., Wichels, A., Garin-Fernandez, A. et al. 2016. Dangerous hitchhikers? Evidence for potentially pathogenic Vibrio spp. on microplastic particles. *Mar. Environ. Res.* 120, 1-8. doi:10.1016/j.marenvres.2016.07.004

Kumar, M., Chen, H., Sarsaiya, S., Qin, S., et al. 2021. Current research trends on micro8 and nano-plastics as an emerging threat to global environment: A review. *J Hazard Mater.*, 409, 124967. doi:10.1016/j.jhazmat.2020.124967.

La Colla, N.S., Botté, S.E., Simonetti, P., Negrin, V.L., et al. 2021. Water, sediments and fishes: First multi compartment assessment of metal pollution in a coastal environment from the SW Atlantic. *Chemosphere*, 282, 131131. doi:10.1016/j.chemosphere.2021.131131

Lee, H.J. 2011. Improving superhydrophobic textile materials. Functional Textiles for Improved Performance, Protection and Health, 339–359. doi:10.1533/9780857092878.33

Lear, G., Kingsbury, J.M., Franchini, S. *et al.* Plastics and the microbiome: impacts and solutions. *Environmental Microbiome* 16, 2 (2021). doi: 10.1186/s40793-020-00371-w

Li, W.C., Tse H.F., Fok L. 2016. Plastic waste in the marine environment: a review of sources, occurrence and effects. *Sci. Total Environ.* 566–567, 333–349. doi: 10.1016/j.scitotenv.2016.05.084.

Li, C., Wang, L., Ji, S., Chang, M., et al. 2021b. The ecology of the plastisphere: Microbial composition, function, assembly, and network in the freshwater and seawater ecosystems. *Water Res.*, 202, 117428. doi:10.1016/j.watres.2021.117428

Li, Y., Zhang, Y., Su, F., Wang, Y., et al. 2022. Adsorption behaviour of microplastics on the heavy metal Cr (VI) before and after ageing. *Chemosphere*, *302*, 134865.https://doi.org/10.1016/j.chemosphere.2022.134865

Liang, C. Y., & Krimm, S. 1958. Infrared spectra of high polymers. VI. Polystyrene. *J. Polym. Sci.* 27(115), 241–254. doi:10.1002/pol.1958.1202711520

Liu, P., Lu, K., Li, J., Wu, X., Qian, L., et al. 2019. Effect of aging on adsorption behavior of polystyrene microplastics for pharmaceuticals: Adsorption mechanism and role of aging intermediates. *J. Hazard. Mater.* 121193. doi:10.1016/j.jhazmat.2019.121193

Liu, S., Huang, J., Zhang, W., et al. 2022. Microplastics as a vehicle of heavy metals in aquatic environments: A review of adsorption factors, mechanisms, and biological effects. *J. Environ. Manage.,* 302, 113995. doi:10.1016/j.jenvman.2021.113995

Liu, Y., Zhang, K., Xu, S., Yan, M., Tao, D. et al. 2021. Heavy metals in the "plastisphere" of marine microplastics: adsorption mechanisms and composite risk. *Gondwana research*. doi : 10.1016/j.gr.2021.06.017

Liu, S., Shi, J., Wang, J., Dai, Y., et al. 2021b. Interactions between microplastics and heavy metals in aquatic environments: a review. *Frontiers in Microbiology,* 12, 730. doi: 10.3389/fmicb.2021.652520

Lu, S., Zhu, K., Song, W., Song, G., et al. 2018. Impact of water chemistry on surface charge and aggregation of polystyrene microspheres suspensions. *Sci. Total Environ.,* 630, 951–959. doi:10.1016/j.scitotenv.2018.02.2

Luna Zaragoza, D., Romero Guzmán, E. T., Reyes Gutiérrez, L.R. 2009. Surface and physicochemical characterization of phosphates vivianite, Fe2 (PO4) 3 and hydroxyapatite, Ca5 (PO4) 3OH. doi:10.4236/jmmce.2009.88052

Luo, H., Li, Y., Zhao, Y., Xiang, Y., et al. 2019. Effects of accelerated aging on characteristics, leaching, and toxicity of commercial lead chromate pigmented microplastics. *Environm. Pollut.,* 113475. doi:10.1016/j.envpol.2019.113475

Luo, H., Xiang, Y., Li, Y., Zhao, Y., Pan, X., 2020. Weathering alters surface characteristic of TiO_2-pigmented microplastics and particle size distribution of TiO_2 released into water. *Sci. Total Environ.,* 729, 139083. doi:10.1016/j.scitotenv.2020.139083

Mahltig, B., 2016. Smart hydrophobic and soil-repellent protective composite coatings for textiles and leather. In Smart composite coatings and membranes (pp. 261-292). Woodhead Publishing. doi:10.1016/B978-1-78242-283-9.00010-5

Mansa, R., and Zou, S. 2021. Thermogravimetric analysis of microplastics: A mini review. Environmental Advances, 5, 100117.doi:10.1016/j.envadv.2021.100117

Mao, R., Lang, M., Yu, X., Wu, R., et al. 2020. Aging mechanism of microplastics with UV irradiation and its effects on the adsorption of heavy metals. *J. Hazard. Mater.,* 122515. doi:10.1016/j.jhazmat.2020.122515

Miao, L., Gao, Y., Adyel, T. M., Huo, Z., et al. 2021. Effects of biofilm colonization on the sinking of microplastics in three freshwater environments. *J. Hazard. Mater.,* 413, 125370. doi:10.1016/j.jhazmat.2021.125370

Monsigny, M., Sene, C., Obrenovitch, A., Roche, A.C., Delmotte, F., Boschetti, E. 1979 Properties of succinylated wheat-germ agglutinin. *Eur. J. Biochem.* 98, 39–45

Murphy, J.A.M.E.S., Riley, J.P. 1962. A modified single solution method for the determination of phosphate in natural waters. Analytica chimica acta, 27, 31-36.

Nava, V., Leoni, B. 2021. A critical review of interactions between microplastics, microalgae and aquatic ecosystem function. *Water Res., 188,* 116476. doi:10.1016/j.watres.2020.116476

Nasrazadani, S., and Hassani, S. 2016. Modern analytical techniques in failure analysis of aerospace, chemical, and oil and gas industries. *Handbook of materials failure analysis with case studies from the oil and gas industry*, 39-54.

Oberbeckmann, S., and Labrenz, M. 2020. Marine Microbial Assemblages on Microplastics: Diversity, Adaptation, and Role in Degradation. *Annu. Rev. Mar. Sci.*, 12(1). doi:10.1146/annurev-marine-010419-010633

Oberbeckmann, S., Kreikemeyer, B., & Labrenz, M. 2018. Environmental factors support the formation of specific bacterial assemblages on microplastics. *Front. Microbiol.*, 8, 2709. doi:10.3389/fmicb.2017.02709

Oberbeckmann, S., Loeder, M.G., Gerdts, G., and Osborn, A.M. 2014. Spatial and seasonal variation in diversity and structure of microbial biofilms on marine plastics in Northern European waters. FEMS microbiology ecology, 90(2), 478-492. doi:10.1111/1574-6941.12409

Oberbeckmann, S., Löder, M.G., and Labrenz, M. 2015a. Marine microplastic-associated biofilms–a review. *Environ. Chem.*, 12, 551-562. doi:10.1071/EN15069

Ocean. (2020, April 02). What Are Microplastics? And Why You Should Care. OER Commons. Retrieved August 307 23, 2020, from https://www.4ocean.com/blogs/blog/what-are-microplastics-and-why-you-should308

Paul-Pont, I., Tallec, K., Gonzalez-Fernandez, C., et al. 2018. Constraints and priorities for conducting experimental exposures of marine organisms to microplastics. *Front. Mar. Sci.*, 5 252. doi:10.3389/fmars.2018.00252

Pazos, R.S., Suarez, J.C., and Gomez, N. 2020. Study of the plastisphere: biofilm development and presence of faecal indicator bacteria on microplastics from the Río de la Plata estuary. *Ecosistemas*, 29(3), 2069. doi:10.7818/ECOS.2069

Payton, T.G., Beckingham, B.A., Dustan, P., 2020. Microplastic exposure to zooplankton at tidal fronts in Charleston Harbor, SC USA. *Estuar. Coast. Shelf Sci.* 232, 106510. doi:10.1016/j.ecss.2019.106510.

Petracci, P. and Sotelo, M. 2013. Aves del estuario del estuario de Bahía Blanca, Una herramienta para su conocimiento y conservación. Bahía Blanca, Argentina: Editorial Muelle Sur.

Pizarro-Ortega, C.I., Dioses-Salinas, D.C., Fernandez Severini, M.D., Forero López, A.D. et al. 2022. Degradation of plastics associated with the COVID-19 pandemic. *Mar. Pollut. Bull*., 113474. doi:10.1016/j.marpolbul.2022.113474

Pretsch, E., Bühlamnn, P., Badertscher, M., 2009. Structure and Determination of Organic Compounds. (4 Eds.) Enlarged edition. p. 17

Raven, J.A., Evans, M.C. and Korb, R.E. 1999. The role of trace metals in photosynthetic electron transport in O2-evolving organisms. Photosynthesis Res. 60, 111–150 (1999).

Rodrigues, A., Oliver, D.M., McCarron, A., and Quilliam, R.S. 2019. Colonisation of plastic pellets (nurdles) by E. coli at public bathing beaches. *Mar. Pollut. Bull.,* 139, 376-380. doi:10.1016/j.marpolbul.2019.01.011

Reisser, J., Shaw, J., Hallegraeff, G., Proietti, M., et al. 2014. Millimeter-sized marine plastics: a new pelagic habitat for microorganisms and invertebrates. PloS one, 9(6), e100289. doi:10.1371/journal.pone.0100289

Rummel, C.D., Jahnke, A., Gorokhova, E., Kühnel, D., Schmitt-Jansen, M., 2017. Impacts of Biofilm Formation on the Fate and Potential Effects of Microplastic in the Aquatic Environment. *Environ. Sci. Technol. Lett.* 4, 258-267. doi: 10.1021/acs.estlett.7b00164

Sandt, C., Waeytens, J., Deniset-Besseau, A., Nielsen-Leroux, C., Réjasse, A., 2021. Use and misuse of FTIR spectroscopy for studying the bio-oxidation of plastics. Spectrochim. *Acta Part A Mol. Biomol. Spectrosc.* 258, 119841. doi: 10.1016/J.SAA.2021.119841

Selenska-Pobell, S., & Merroun, M. 2010. Accumulation of Heavy Metals by Micro-organisms: Biomineralization and Nanocluster Formation. In Prokaryotic cell wall compounds (pp. 483-500). Springer, Berlin, Heidelberg.

Silva, M.M., Maldonado, G.C., Castro, R.O., de Sá Felizardo, J., Cardoso, R.P., et al. 2019. Dispersal of potentially pathogenic bacteria by plastic debris in Guanabara Bay, RJ, Brazil. *Mar. Pollut. Bull.*, 141, 561-568. doi: 10.1016/j.marpolbul.2019.02.064

Speake, M.A., Carbone, M.E. Spetter, C.V. 2018. Ocurrencia de eventos de emergencia ambiental en el área costera de Bahía Blanca, provincia de Buenos Aires. En Libro de resúmenes de las XII Jornadas Nacionales de Geografía Física (pp. 91-95). Argentina: Bahía Blanca. Recuperado de https://redargentinadegeografiafisica.files.wordpress.com/2018/04/resc3bamenes-xiijngf-2018.pdf

Spetter, C.V., 2006. Ciclo biogeoquímico de nutrientes inorgánicos de nitrógeno en los humedales del estuario de Bahía Blanca. Bahía Blanca, Argentina: Universidad Nacional del Sur (Doctoral dissertation, Ph. D dissertation).

Spetter, C.V., Buzzi, N.S., Fernández, E.M., Cuadrado, D.G., and Marcovecchio, J.E. 2015. Assessment of the physicochemical conditions sediments in a polluted tidal flat colonized by microbial mats in Bahía Blanca Estuary (Argentina). *Mar. Pollut. Bull.* 91(2), 491–505. doi:10.1016/j.marpolbul.2014.10.

Sudhakar, M., Priyadarshini, C., Mukesh D., Sriyutha Murthy, P., et al. 2007. Marine bacteria mediated degradation of nylon 66 and 6. , 60(3), 144–151. doi:10.1016/j.ibiod.2007.02.002

Sussarellu, R., Suquet, M., Thomas, Y., Lambert, C., et al. 2016. Oyster reproduction is affected by exposure to polystyrene microplastics. *Proc. Natl. Acad. Sci. U.S.A.* 113, 2430–2435. doi: 10.1073/pnas.1519019113

Suresh, K., Kumar, R.V., Kumar, M. et al. 2017. Sonication-assisted synthesis of polystyrene (PS)/organoclay nanocomposites: influence of clay content. *Appl Nanosci* 7, 215–223 doi:10.1007/s13204-017-0562-2

Sturm, M.T, Schuhen, K, Horn, H. 2021. Method for rapid biofilm cultivation on microplastics and investigation of its effect on the agglomeration and removal of microplastics using organosilanes. Sci Total Environ. 151388. doi: 10.1016/j.scitotenv.2021.151388.

Tang, S., Lin, L., Wang, X., Feng, A., & Yu, A. 2020. Pb (II) uptake onto nylon microplastics: interaction mechanism and adsorption performance. *J. Hazard. Mater.*, 386, 121960. doi:10.1016/j.jhazmat.2019.121960

Tang, S., Lin, L., Wang, X., Yu, A., Sun, X., 2021. Interfacial interactions between collected nylon microplastics and three divalent metal ions (Cu(II), Ni(II), Zn(II)) in aqueous solutions. *J. Hazard. Mat.*, 123548. doi:10.1016/j.jhazmat.2020.123548.

Thompson R.C. 2015. Microplastics in the marine environment: sources, consequences and solutions. In: Marine anthropogenic litter. *Springer, Cham*, 185–200. doi:10.1007/978-3-319-16510 -3_7

Truchet, D.M., Forero López, A.D., Ardusso, M.G., Rimondino, G.N., et al. 2021b. Microplastics in bivalves, water and sediments from a touristic sandy beach of Argentina. *Mar. Pollut. Bull.*, 173, 113023. doi:10.1016/j.marpolbul.2021.113023

Truchet, D.M., Buzzi, N.S., Negrin, V.L., et al. 2022a. First long-term assessment of metals and associated ecological risk in subtidal sediments of a human-impacted SW Atlantic estuary. *Mar. Pollut. Bull.*, 174, 113235. doi:10.1016/j.marpolbul.2021.113235

Truchet D.M., Ardusso M.G., Forero-López A.D., Rimondino G.N., Buzzi N.S. et al. 2022b Tracking synthetic microdebris contamination in a highly urbanized estuary through crabs as sentinel species: an ecological trait-based approach. *Sci. Total Environ.* (under review).

Turner, A., Holmes, L.A., 2015. Adsorption of trace metals by microplastic pellets in fresh water. *Environ. Chem.* 12, 600-610. doi:10.1071/EN14143

Verma, S., & Kuila, A. 2019. Bioremediation of heavy metals by microbial process. *Environmental Technology & Innovation, 14*, 100369.

Villagrán, D.M., Fernandez-Severini, M.D., Biancalana, F., et al., 2019. Bioaccumulation of heavy metals in mesozooplankton from a human-impacted south western Atlantic estuary (Argentina). *J. Mar. Res.* 77, 217–241. doi:10.1357/002224019826887362.

Villagran, D.M., Truchet, D.M., Buzzi, N.S., Forero-Lopez, A.D., et al. 2020. A baseline study of microplastics in the burrowing crab (Neohelice granulata) from a temperate southwestern Atlantic estuary. *Mar. Pollut. Bull.*, 150, 110686. doi:10.1016/j.marpolbul.2019.110686

Villagrán, D.M., 2019b. Dinámica de metales pesados en el material particulado en suspensión y plancton en ambientes costeros afectados por descargas de origen antrópico. Ph.D. thesis. Universidad Nacional del Sur, p. 151. http:// repositoriodigital.uns.edu.ar/handle/123456789/4602

Wang, Z., Cao, J., Meng, F., 2015. Interactions between protein-like and humic-like components in dissolved organic matter revealed by fluorescence quenching. *Water Res.*, 68, 404–413. doi:10.1016/j.watres.2014.10.024

Wang, J., Peng, J., Tan, Z., Gao, Y., et al. 2017. Microplastics in the surface sediments from the Beijiang River littoral zone: Composition, abundance, surface textures and interaction with heavy metals. *Chemosphere*, 171 248–258. doi:10.1016/j.chemosphere.2016.12

Wu, X., Pan, J., Li, M., Li, Y., Bartlam, M., and Wang, Y. 2019. Selective enrichment of bacterial pathogens by microplastic biofilm. *Water Res., 165*, 114979.doi: 10.1016/j.watres.2019.114979

Wu, C., Tanaka, K., Tani, Y., et al. 2022. Effect of particle size on the colonization of biofilms and the potential of biofilm-covered microplastics as metal carriers. *Sci. Total Environ.*, 821, 153265. doi:10.1016/j.scitotenv.2022.153265

Xie, H., Chen, J., Feng, L., He, L., et al. 2021. Chemotaxis-selective colonization of mangrove rhizosphere microbes on nine different microplastics. *Sci. Total Environ.*, 752, 142223. doi:10.1016/j.scitotenv.2020.142223

Xie, Q., Li, H., Li, Z., Zhang, H., et al. 2022. Accumulation, chemical speciation and ecological risks of heavy metals on expanded polystyrene microplastics in seawater. *Gondwana Research.* 108, 181-192. doi:10.1016/j.gr.2022.01.017

Xu, X., Wang, S., Gao, F., Li, J., et al. 2019. Marine microplastic-associated bacterial community succession in response to geography, exposure time, and plastic type in China's coastal seawaters. *Mar. Pollut. Bull.* 145, 278-286. doi:10.1016/j.marpolbul.2019.05.036

Yao, S., Cao, H., Arp, H.P.H., Li, J., et al. 2021. The role of crystallinity and particle morphology on the sorption of dibutyl phthalate on polyethylene microplastics: Implications for the behavior of phthalate plastic additives. *Environ. Pollut.*, 283, 117393. doi:10.1016/j.envpol.2021.117393

Zardus, J.D., Nedved, B.T., Huang, Y., Tran, C., and Hadfield, M.G. 2008. Microbial biofilms facilitate adhesion in biofouling invertebrates. *The Biological Bull.*, 214(1), 91-98.

Zhang, B., Yang, X., Liu, L., Chen, L., et al. 2021. Spatial and seasonal variations in biofilm formation on microplastics in coastal waters. *Sci. Total Environ.*, 770, 145303. doi:10.1016/j.scitotenv.2021.145303

Zhao, Y., Gao, J., Zhou, X., Li, Z., Zhao, C., et al. 2023. Bio-immobilization and recovery of chromium using a denitrifying biofilm system: Identification of reaction zone, binding forms and end products. *J. Environ. Sci. 126*, 70-80. doi:10.1016/j.jes.2022.03.050

Zhou, Z., Sun, Y., Wang, Y., et al. 2022. Adsorption behavior of Cu (II) and Cr (VI) on aged microplastics in antibiotics-heavy metals coexisting system. *Chemosphere, 291*, 132794. doi.org/10.1016/j.chemosphere.2021.132794

Zettler, E.R., Mincer, T.J. and Amaral-Zettler, L.A. 2013. Life in the 'plastisphere': microbial communities on plastic marine debris. *Environ. Sci. Technol.* 47, 7137–7146. doi:10.1021/es401288x

Table 1. Correlation matrix with the significant correlations detected between heavy metals of the plastisphere on Ny and PSMPs and some of the physicochemical variables like SPR (soluble reactive phosphorus), Chl-*a,* and TPC (total particulate carbon) of the water column at Cuatreros Port (CP).

	Cr-NyMPs	Cr-PSMPs	Mn-NyMPs	Mn-PSMPs	Cu-NyMPs	Cu-PSMPs	Zn-NyMPs	Zn-PSMPs	Cd-NyMPs	Cd-PSMPs	Pb-NyMPs	Pb-PSMPs
Chl-a			-0.81*	-0.81*								
TPC					0.87*		0.87*					
SPR												0.77*
Cr-NyMPs	**1**											
Cr-PSMPs	1.0***	**1**										
Mn-NyMPs	0.90**	0.89**	**1**									
Mn-PSMPs	0.83*	0.82*	0.94***	**1**								
Cu-NyMPs					**1**							
Cu-PSMPs	0.86**	0.86**	0.96***	0.92**		**1**						
Zn-NyMPs					0.99***		**1**					

Zn-PSMPs								**1**			0.71*	
Cd-NMPs	0.93***	0.93***	0.97***	0.89**		0.94***			**1**	0.79*		
Cd-PMPs			0.85**	0.94***		0.90**				**1**		
Pb-NyMPs											**1**	

Table 2. Comparison of heavy metal levels found in the plastisphere on MPs in this study area and in other regions of the world (μg.g^{-1}). Historical level data of heavy metals in suspended particulate matter (SPM) and surface waters from the assay zone (CP). Data presented in ranges (minimum-maximum) and mean (± SD) of heavy metals levels in the plastisphere on MPs.

Sample	**Location**	**Cr** **μg.g^{-1}**	**Mn** **μg.g^{-1}**	**Zn** **μg.g^{-1}**	**Cu** **μg.g^{-1}**	**Cd** **μg.g^{-1}**	**Pb** **μg.g^{-1}**	**Reference**
Plastisphere NyMPs	**Cuatreros Port (CP)** Bahía Blanca estuary (Argentina)	range (<0.03-1638.36) 345.86± 722.64	range (80.53-885.67) 295.82 ± 269.0	range (14.88-319.04) 80.25 ± 107.22	range (1.68-255.97) 44.15 ± 93.77	range (<MDL-14.81) 6.39 ± 5.78	range (<0.02-29.51) 17.10 ± 11.16	In this study (assay)
PSMPs		range (<0.03-2403.6) 415.54± 973.99	range (145.81-698.4) 326.10 ± 181.5	range (7.34-43.17) 24.41 ±11.18	range (1.30-12.04) 8.79 ± 7.07	range (1.40-10.20) 5.60 ± 2.85	range (MDL-21.91) 8.58 ± 6.97	
Surface waters	**Cuatreros Port (CP)**	range 0.29-						

		0.61µg.L						
SPM	Bahía Blanca estuary (Argentina) **Cuatreros Port (CP)**	mean: 3.15 ± 1.02 µg.g^{-1}	mean: 123.5 ± 4.94 µg.g^{-1}	mean: 103.5 ± 37.48 µg.g^{-1}	mean: 46.35 ± 5.02 µg.g^{-1}	<MDL	mean: 2.5 ± 0.84 µg.g^{-1}	Forero-López et al. 2021a
		range (11.20-16.49) 13.2 ± 2.24 µg.g^{-1}	range (424.7-668) 548.5 ± 99 µg.g^{-1}					Forero-López et al. 2021b
		15.22 ± 5.06 µg.g^{-1}	558.8 ± 148.2 µg.g^{-1}	7.70 ± 5.22 µg.g^{-1}	19.40 ± 5.03 µg.g^{-1}	0.37 ± 0.30 µg.g^{-1}	60.98 ± 14.6 µg.g^{-1}	Villagrán et al. (2019b)
Surface waters	**Cuatreros Port (CP)**	1.66-18 µg.L				0.060-0.56 µg.L	MDL-54 µg L	La Colla et al. (2021)
Plastisphere PS/PE/PP surface waters	Zhujiang Hong Kong µgg^{-1}	range (11.1-89.9) mean: 29.85 µgg^{-1}	range (76.9-326) mean: 193 µgg^{-1}	range (47.9-514) mean: 160 µgg^{-1}	range (8.76-1,217) mean: 237 µgg^{-1}	range (0.16-4.48) mean: 1.10 µgg^{-1}	range (8.71-83.4) mean: 29.3 µgg^{-1}	Liu et al. (2021)
PE and PET found in sediments	East Kolkata Wetland (India)	range (26.26–342.28 µgg^{-1})		range (1.88–1191.5 µgg^{-1})	range (0.29–119.59 µgg^{-1})		range (0.04–104.63 µgg^{-1})	Sarkar et al. (2021)

Credit Author Statement

A.D. Forero-López: Conceptualization, Data curation, Formal analysis, Investigation, Visualization, Methodology, Supervision,Writing - original draft, Formal Analysis, Writing - review & editing.

L.I. Brugnoni: Methodology, Resources, Writing - original draft, Visualization, Writing- reviewing & editing,

B. Abasto: Methodology**,** Writing - original draft, Writing- reviewing & editing,

G.N. Rimondino: Conceptualization, Data curation, Formal analysis, Methodology, Writing - original draft, Writing - review & editing.

V.L. Lassalle: Methodology**,** Writing - original draft, Writing - review & editing.

M.G. Ardusso: Methodology**,** Writing - original draft, Writing - review & editing.

M.S. Nazzarro: Methodology, Writing - original draft, Writing - review & editing.

A.M. Martinez: Methodology**,** Writing - original draft, Writing - review & editing.

C.V. Spetter: Methodology**,** Visualization, Writing- reviewing & editing, Resources, Funding acquisition.

F. Biancalana: Methodology, Visualization, Writing - original draft, Writing - review & editing.

M.D. Fernández-Severini: Conceptualization, Methodology, Investigation, Writing - original draft, Supervision, Writing - review & editing, Resources, Project administration, Formal Analysis, Funding acquisition.

Environmental Implication”

The manuscript is of environmental relevance because it studies the presence of hazardous materials like microplastics and heavy metals in a marine ecosystem and their interactions with microorganisms of human health implications. Microplastics produce several impacts on the environment and one of them is the formation of the plastisphere: microorganisms that colonize plastics. This study showed that MPs surfaces acted as new niches for heterotrophic microorganisms like pathogenic bacteria and favored the adsorption of heavy metals, with potential migration through the water to other marine ecosystems. Thus, the plastisphere plays as a metal vector with impacts on both aquatic biota and humans, through the food webs.

Declaration of interests

☒The authors declare that they have no known competing financial interests or personal relationships that could have appeared to influence the work reported in this paper.

☐The authors declare the following financial interests/personal relationships which may be considered as potential competing interests:

Highlights

- **Pathogenic bacteria were identified on the Ny and PS-microplastic surfaces.**
- **Superficial weathering and leaching of TiO_2 from Ny Microplastics were evidenced.**
- **The crystallinity of Ny-microplastics decreased during the assay.**
- **High Cr, Mn, and Zn levels were detected on the microplastic surface biofilms.**